



REPORT

AN ENGINEERING ASSESSMENT OF THE CURRENT STABILITY OF THE PILLAR MOUNTAIN SLIDE

KODIAK, ALASKA

Submitted To: Glenn Melvin
City of Kodiak
PO Box 1397
Kodiak, AK 99615

Submitted By: Golder Associates Inc.
2121 Abbott Road, Suite 100
Anchorage, AK 99507

Distribution:
1 PDF Copy – City of Kodiak
2 Copies – Golder Associates Inc.

November 20, 2013

13-00823





Table of Contents

1.0	INTRODUCTION.....	1
1.1	Pillar Mountain Slide History	1
2.0	LIDAR ACQUISITION AND USE IN ANALYSES	3
2.1.1	Terrain Model Developed from LiDAR Data	3
2.1.2	Georeferencing the LiDAR.....	3
2.1.3	Terrain Model Used to Develop Cross Sections for Numerical Modelling.....	4
3.0	2013 GROUND RECONNAISSANCE	5
3.1	Reconnaissance Performed in September 2013	5
3.2	No Significant Changes Were Observed	5
3.3	Active Rockfall Continues	6
4.0	GEOLOGICAL MODEL.....	7
4.1	Site Geology.....	7
4.2	Envisaged Failure Mechanism	8
4.2.1	Structural Geology Favorable for Kinematic Stability	8
4.2.2	Pre-1971 Quarrying at Toe Possibly Initiated Toppling	8
4.3	Estimated Material Properties based on Field Observations.....	9
5.0	NUMERICAL ANALYSIS	10
5.1	Introduction.....	10
5.2	Back Analysis.....	10
5.3	Shallow and Global Failure Analysis.....	11
5.3.1	Shallow Failure Analysis	11
5.3.2	Global/Deep Seated Analysis	12
5.3.3	Results Summary (Shallow and Deep Seated Failure)	12
6.0	DISCUSSION AND CONCLUSIONS FROM SITE RECONNAISSANCE AND MODELING	14
6.1	Relative Probability of Failure	14
6.2	Progressive Nature of Failure and Importance to Future Instability Predictions.....	15
6.3	Stability of the Upper Head Scarp.....	15
6.4	Seismic Considerations.....	16
6.5	Stability of Flatter Slopes Adjacent to 1971 Failure	16
6.6	Global Failure	16
7.0	SUMMARY OF CONCLUSIONS	18
8.0	RECOMMENDATIONS.....	19
9.0	CLOSURE.....	20
10.0	REFERENCES.....	21



List of Tables

Table 1	Ranges of Assumed Factored Rock Mass Strength Values for Back Analyses
Table 2	A Summary of Analysis Types and Cross Sections Used
Table 3	Shear Strength Reduction Method Results Summary for Various Analyses
Table 4	Relative Risk Comparison for Various Failure Modes at Pillar Mountain

List of Figures

Figure 1	Vertical Colorized LiDAR Image of Pillar Mountain Slide
Figure 2	Oblique Bare Earth View of Slide Area Using Hillshade from LiDAR Data
Figure 3	Kodiak Air Temperatures in 1971
Figure 4	Looking West at the LiDAR Terrain Model
Figure 5	Ground Distance Measurement on LiDAR Model
Figure 6	Area Covered Targeted in LiDAR Survey
Figure 7	Three Cross Sections Selected for Numerical Analyses
Figure 8	Profiles of Cross Sections from LiDAR Model
Figure 9	2001 Aerial Photo
Figure 10	2013 LiDAR Image of the Slide
Figure 11	Upslope View of Slide Area (September 21, 2013)
Figure 12	View Downslope from Head-scarp (September 21, 2013)
Figure 13	View of Northeast Side of Slide Area (September 21, 2013)
Figure 14	Toe of Talus Cone with Gabion Wall to the Left (September 21, 2013)
Figure 15	View of Upper Slope Terrain Above the Head Scarp (September 21, 2013)
Figure 16	Gabion Wall Distorted by Rockfall Impacts (September 21, 2013)
Figure 17	Rockfall across Road and Impact Craters on Pavement (September 21, 2013)
Figure 18	Larger Rocks Retained by Gabion Wall
Figure 19	Typical Head Scarp Rock Structure
Figure 20	Rock Bedding and Jointing in Head Scarp
Figure 21	Cross Slope View of Head Scarp Rock Structure
Figure 22	Rock Structure and Talus
Figure 23	Conceptual Model of Joints 1 and 2
Figure 24	Schematic Illustrating Tensile Failure Mechanism
Figure 25	Example of Typical and Elevated Water Tables Shown for Section 4
Figure 26	Close Up Example of Mesh Setup and Jointing
Figure 27	Tensile Fracturing/Yielded Element Progression to Failure (1 of 4) for Over Steepened Section 6
Figure 28	Tensile Fracturing/Yielded Element Progression to Failure (2 of 4) for Over Steepened Section 6
Figure 29	Tensile Fracturing/Yielded Element Progression to Failure (3 of 4) for Over Steepened Section 6
Figure 30	Tensile Fracturing/Yielded Element Progression to Failure (4 of 4) for Over Steepened Section 6
Figure 31	Model Tensile Fracturing and Section 6 on Total Slope Profile
Figure 32	Model Back Analyses for Section 6 Showing Calculated Failure Zone
Figure 33	Tensile Fracturing/Yielded Element Progression to Failure (1 of 5) for Over Steepened Section 4
Figure 34	Tensile Fracturing/Yielded Element Progression to Failure (1 of 5) for Over Steepened Section 4
Figure 35	Tensile Fracturing/Yielded Element Progression to Failure (3 of 5) for Over Steepened Section 4
Figure 36	Tensile Fracturing/Yielded Element Progression to Failure (4 of 5) for Over Steepened Section 4
Figure 37	Tensile Fracturing/Yielded Element Progression to Failure (5 of 5) for Over Steepened Section 4



- Figure 38 Cross Section 4 Failure Zone
Figure 39 Model Run for Global Failure Cross Section 4 (shear failure indicated by red 'x')
Figure 40 Calculated Displacement Contours for Cross Section 4 (color contours shown only to indicate total failure zone)

List of Appendices

- Appendix Pillar Mountain Slide Zone - Final Report – Kodiak Mapping Inc.



1.0 INTRODUCTION

The City of Kodiak retained Golder Associates (Golder) to conduct an updated slope stability assessment of the Pillar Mountain slide area located along Rezanof Drive approximately one mile west of downtown Kodiak as shown in the colorized LiDAR images in Figures 1 and 2. The purpose of this new assessment was to assist the City in understanding the potential for future slope failures and help quantify the risks associated with future slides as they may impact the ongoing Pier 3 Development Project. To accomplish this work Golder performed the following tasks:

- Acquired and analyzed LiDAR imagery of the slide area
- Performed a geologic reconnaissance of the Pillar Mountain Slide Area
- Performed stability analyses of the slope using numerical modeling to incorporate rock structure
- Prepared this geologic/engineering report presenting our findings

1.1 Pillar Mountain Slide History

In December of 1971 a large slide occurred on Pillar Mountain. The slide started on December 5 and slides continued throughout December. By the end of December, it was estimated that 600,000 yards of material had fallen (R&M, 1982). The flanks of Pillar Mountain have been used as a source of borrow for decades. Prior to the 1971 Slide, a bedrock exposure with active rockfall existed at the present toe of the slide area. The 1971 slide area was about 300 feet high and 1,400 feet long. In 1971 a quarry was developed along the abandoned highway at an elevation of approximately 125 feet. Approximately 300,000 cubic yards of material was mined prior before large amounts of rock debris began falling from a vertical gully in the slope. During the 1971 slide extensive development of open transverse ground fractures were noted on the slope above the slide. Activity since 1971 has remained low with small showers of rock and occasional large blocks intermittently falling from the over steeped back scarp of the slide area. At the time of the 1982 investigations, many of the upslope ground features were partially to completely filled with slope wash soils and were revegetated. However, some fractures still appeared open and fresh (R&M, 1982). The Pillar Mountain Slide encompasses an area approximately 1,200 feet high and 1,700 feet wide situated above West Rezanof Drive.

The 1982 report stated that a sudden catastrophic failure of the slide into St. Paul Harbor could send a damaging wave into the Kodiak waterfront similar in size to the 1964 seismic sea waves that devastated the city following the 1964 earthquake. The 1971 slide was large, but took almost month for the major slides to stop. It started near the toe as rockfall into an active quarry. It did not produce any recorded waves in St. Paul Harbor.

The 1964 earthquake epicenter was approximately 300 miles from Kodiak and that while Kodiak was subjected to a tsunami as a result of the earthquake; there are no known reports of large or unusual



rockfalls on Pillar Mountain during this major event. During the earthquake, the City experienced over 2 minutes of strong ground motions which made walking difficult. This does imply that the slope was subjected to significant shaking for 2 minutes or more. Earthquakes are frequent in the Kodiak area and several Richter Magnitude 6 or larger earthquakes have occurred in the area since 1964.

The 1982 report stated "Several springs at the east margin of the rockfall are apparently discharging water from a thrust fault dipping into the mountain." They also mentioned springs they identified in 1962 aerial photography that have since been covered by talus.

The air temperatures in Kodiak for 1971 are shown in Figure 3. This figure shows that there was a significant cold spell in late November before the slide started in early December. This will be discussed later in this report. 2002 Investigation.

In November 2002, Golder Associates reviewed existing information on the slide, interpreted and compared sets of stereo-pairs of aerial photographs taken in 1983 and 2001, flew over the site to take low level oblique photographs, and conducted a field traverse around the entire slide area. The purpose of this effort was to assess any visible changes compared to the 1982 study. This reconnaissance effort found that the slide area was continuing to discharge rockfall in fairly random small releases from the head scarp of the 1971 slide rather than large catastrophic failures. Changes to the slide and upper slope in the intervening 20 years were relatively minor and generally limited to slow upward progression of the active rockfall due to raveling. Although there were numerous transverse ground cracks on the upper slopes, they were heavily overgrown and/or partially filled with soil and organics. There was no apparent evidence of significant ongoing deep-seated movement.

No evidence of spring activity was noted in this investigation. However, the photography did show the vegetation variations on the slope which are likely related to the proximity of ground water to the surface. The bushy and darker green areas are likely wetter than the more barren terrain.



2.0 LIDAR ACQUISITION AND USE IN ANALYSES

Light detection and ranging (LiDAR) is a remote sensing technology that measures distance by illuminating a target with a laser and analyzing the reflected light. This technology was used to establish an elevation base for future monitoring of the slope surface and to provide a terrain model that could be used in our numerical and visual analyses. As detailed further in Appendix A, “LiDAR and Digital Imagery were simultaneously acquired on 18 July 2013 to produce a LiDAR derived Bare Earth Surface in LAS format with approximately 45 – 75 points per meter. Point Density varies throughout the project with more emphasis given to the scar and the steeper faces of the slope.”

The points in the LiDAR were classified according to the ASPRS Standard Point Classes set by American Society for Photogrammetry and Remote Sensing (ASPRS). The digital Imagery Terrain model was utilized to support the orthorectification and generation of a 1.5-inch pixel orthophoto. The resulting orthophoto was also utilized during the LiDAR classification process to help visually differentiate between rock, soil, and vegetation.

The data acquired can to be utilized as a baseline surface for ground surface change detection analysis of the Pillar Mountain slide vicinity. Future datasets can be compared to the baseline model to determine and measure any significant shifts in geological features or orientations.

2.1.1 *Terrain Model Developed from LiDAR Data*

The LiDAR data was used to create a terrain surface model. Using Quick Terrain Reader© (QTR) and Quick Terrain Modeler© (QTM) software this terrain model can be used to create a topographic base for numerical modeling and for visual evaluations. Figures 1, 2, and 4 were all produced by using QTR to rotate and move the model so that side, front, straight on, and vertical down views of the slide area could be viewed and evaluated. In addition with QTM the terrain model can be cut to produce cross sectional views wherever desired in the model. Additional software used for processing and analyzing the LiDAR data include Globalmapper v15, and Civil3D 2013.

Figures 1 and 4 are colorized images made by taking the LiDAR Bare Earth image (shown in Figure 2) and matching the digital orthophoto color pixels to the Bare Earth Points to add the color.

2.1.2 *Georeferencing the LiDAR*

The Bare Earth model surface is a representation of the ground surface consists of a series of points classified as Ground each of which has a specific coordinate within the model. This LiDAR was georeferenced using airborne GPS data during acquisition which was corrected by Kodiak CORS (Continuously Operating Receiving Stations). Specific points on the Bare Earth model can be identified on the ground surface. These points were surveyed and tied to the Alaska State Plane Coordinate System. Once this was done each point in the model had a location associated with the Alaska State Plane



Coordinate System. The model can also be used to measure distances between points as shown in Figure 5. In this figure the measurement line shows a length of 48.16 feet on the slope. In the upper right corner of the figure a colored axis shows the orientation of the model when the image shown was produced. The blue line shows the vertical position and the red and green lines show the compass directions based on the referenced coordinates of the model.

2.1.3 Terrain Model Used to Develop Cross Sections for Numerical Modelling

In our analyses of the slide slope a number of cross sections were developed from the LiDAR data. The area covered by the LiDAR data acquisition is shown in Figure 6. Figure 7 shows the locations of the 3 cross sections used in our analyses. Figure 8 shows profiles of the cross sections cut along the three locations shown in Figure 7.



3.0 2013 GROUND RECONNAISSANCE

The purpose of the new reconnaissance was to observe the current conditions at the slide to assess any visible changes compared to the conditions observed in our previous reconnaissance in November, 2002. The 2002 reconnaissance was documented in a report by Golder (November 14, 2002) with the purpose of assessing visible changes in the slide area as described in the July 1982 Pillar Mountain Slope Stability Study, Final Project Report prepared for the City of Kodiak by (R&M, 1982).

The reconnaissance was conducted in September 2013 by Robert Dugan, an engineering geologist, who also conducted the 2002 reconnaissance. The September 2013 reconnaissance included the following:

- Review of the July 1982 Pillar Mountain Slope Stability Study.
- Review of the Golder November 2002 Report – Pillar Mountain Slide Reconnaissance.
- Interpretation of new LiDAR imagery taken by Kodiak Mapping Inc.
- Field traverses of the slide vicinity to observe evidence of recent movement (such as slides, fresh scarps, tension cracks, and rockfall accumulations).
- Review the rock conditions with a view to providing input into the modeling.

3.1 Reconnaissance Performed in September 2013

The ground reconnaissance was conducted on September 21, 2013. The reconnaissance was preceded by the interpretation of preliminary LiDAR data that had been modeled in Bare Earth using the QTM. The LiDAR data, obtained from Kodiak Mapping Inc., had fairly high resolution with approximately 45 to 75 points per meter. The modeled LiDAR data allowed us to look at the slide in 3-D from any angle and from any distance, as if one were in a helicopter. Figures 1, 2, and 4 show LiDAR images of the slide made using the QTM or the QTR. A LiDAR image of the slide area showing the active rockfall zone, talus accumulation, prominent lineaments, and the recon route is shown in Figure 2.

3.2 No Significant Changes Were Observed

The slide area exhibited no significant changes from the conditions observed in 2002. Figure 9 shows a photograph taken in 2001. Figure 10 shows a similar view in LiDAR taken in 2013. Numerous photographs were taken on September 21, 2013. Several are presented as figures which are described as follows:

- Figure 11 was taken from the toe of the current talus pile looking to the top of the slope. It shows relatively uniform sized talus sloping up to a series of head scarps.
- Figure 12 was taken near the top of one of the head scarps looking towards downtown Kodiak. It shows some of the rock structure and the steepness of the terrain.
- Figure 13 is a good view of the talus below a head scarp.
- Figure 14 shows the talus collecting at the gabion wall protecting the highway.
- Figure 15 shows the grassy terrain on the top of the slope above the head scarps.



- Figures 16 and 18 show the condition of the gabion wall and the accumulation of talus behind it.
- Figure 17 shows impact craters in the highway pavement and talus under the guard rail across the highway from the gabion wall.
- Figures 19 through 22 show the rock structure in the head scarp above the talus slope.

The bedrock in the active rockfall area (head scarp) is steep and fractured and appears to be continuing to discharge the occasional rock, or small group of rocks, some of which reach to toe of the large talus slope as can be seen in the photographs in Figures 11 through 14. The rockfall is largely attributable to freeze-thaw and frost jacking. The prominent lineaments are heavily vegetated (See Figure 16) and no fresh cracking of the ground beside or above the slide area was observed. There was no new evidence of deep-seated movement.

3.3 Active Rockfall Continues

The highway below the slide is protected from rockfall by a ditch and gabion wall which can be seen in Figure 17. As the figure shows, the gabion wall is distorted in places by apparent rockfall impacts. A couple rocks appeared to have reached the highway and possibly reached the far guardrail as is evident in Figure 18. Some of the largest blocks (See Figure 19.) reached the gabion wall and these are typically tabular and weigh 50-200 pounds. They apparently begin spinning on edge after they fall and thereby achieve greater velocity enroute down the talus cone compared to rocks that fall and slide. The talus is composed of larger blocks, typically in the 10-50 pound range, on the southwest side of the cone, while the northeast side of the cone is typically characterized by blocks in the 1-5 pound range. The talus cone has grown slightly but there are no large blocks ($>0.25 \text{ yd}^3$) evident in the talus accumulations.



4.0 GEOLOGICAL MODEL

4.1 Site Geology

The ground reconnaissance observations and review of previous information were used to assess and summarize the geology at the Pillar Mountain site. This knowledge provided insight to developing an understanding of the likely failure mechanism that precipitated the 1971 slide. It is believed that envisioning a failure mechanism is key to understanding the potential for future failures and whether they could be small-scale or large-scale slides.

The bedrock and Pillar Mountain has been mapped by the U.S. Geological survey as dark-grey to black fine-grain slate and argillite to phyllite with lesser amounts of greywacke (Late Cretaceous Kodiak Formation). Individual beds of phyllite are described to be 1 inch to 12 inches in thickness with the more massive beds of argillite or greywacke beds reported to be up to 20 feet thickness (Kachadoorian and Slater, 1978 and R&M, 1981). Photographs in Figures 19 through 22 were taken during the reconnaissance and show typical bedding features above the talus on the slope.

The geological conditions at Pillar Mountain can be summarized as follows (based on both field observation and the bedding and joint set orientations described in the 1978 Kachadoorian and Slater report prepared by the U.S. Geological Survey):

- Bedding described to dip at an angle ranging from 40-70 degrees toward 295-310 degrees (northwesterly dipping into the slope).
- Other jointing described to crosscut bedding includes:
 - J1 joint set steeply dipping at 70-90 degrees toward 128-138 degrees (southeasterly dip and strike sub-parallel to the slope contours).
 - J2 joint set, which is conjugate to set J1, was described as oscillating on either side of vertical with a dip direction close to 160 or 340 degrees (either northwest dipping or south east dipping).
 - J3 joint set was described to dip steeply between 75-80 degrees toward 015-030 (northeast dipping into the slope).
 - J4 joint set was described to dip steeply from 68-90 degrees toward 223-234 (southwest dip which strikes obliquely across the slope).

The steeply dipping J1 and J2 joint set orientations also appear to be sub-parallel to a few of the main lineament orientations observed in the air photos and LiDAR images. These two joint sets are approximately 30 degrees apart in dip direction. In Figure 23 models of slope surfaces have been shown as plates and draped with a surface similar to the actual slope to aid in visualizing their potential interactions.



The R&M geological report also notes two additional poorly developed joint orientations near the toe of slope that were not previously mapped or noted by Kachadoorian and Slater. R&M noted that these sets (described in the 1982 R&M report as Set E and Set F) dip at an angle of roughly 25-30 degrees in a southerly direction. i.e., they dip out of the slope. If these joint sets were pervasively developed throughout the slope, it is anticipated that planar sliding (on joints dipping out of the slope) would be the dominant failure mechanism and the same joint set would be observed in the weathered head scarp of the 1971 failure. Since this does not appear to be the case, the additional jointing noted by R&M is not considered to be significant in term of failure on the scale of the mountain.

4.2 Envisaged Failure Mechanism

Based on the assessed structural geology of the site and field observations there are no strong indications that the failure mechanism at Pillar Mountain is a typical planar-type failure or translational sliding on a preexisting fault or weak surface that dips out of the slope.

4.2.1 Structural Geology Favorable for Kinematic Stability

In general, the structural geology of the Pillar Mountain site, as mapped by others and observed in the field by Golder, appears to be favorable from a kinematic stability perspective, i.e. there is little or no potential for the rock mass to slide down the hill on unfavorably orientated joints. This is due to the fact that bedding is dipping into the slope and the other joint sets that cross cut bedding are steep to sub vertical in nature and do not daylight unfavorably in the slope. For a failure to propagate as a translation slide or on a planar or circular sliding surface, shearing would need to occur through intact rock at an orientation that is near-perpendicular to bedding and the other sub-perpendicular joint sets and this is considered to be highly unlikely. It is much more likely that failure has been induced initially by tensile failure or snapping of sheets or rock delineated by bedding. Once the tensile fractures start to coalesce at the base of the toppling sheets of rock and relative slippages start to occur on the bedding planes it is possible to envisage a broken surface at the base of the broken pillars on which downslope movement could occur. This mechanism could be considered analogous to cracking occurring at the base of a leaning pillar due to induced moments and is also more likely because the tensile strength of intact rock is in the order of ten times less than the shear strength of the rock in the slope. The broken surface, resulting from coalescing tensile fractures, along which shearing can occur, will be weaker than any assumed circular (or similar) surface on which shearing has to occur through intact rock (i.e. shearing perpendicular to bedding). Tensile crack formation for toppling beds is shown schematically in Figure 24.

4.2.2 Pre-1971 Quarrying at Toe Possibly Initiated Toppling

It is envisaged that with the removal of toe support and over steepening that occurred during quarrying activity pre-1971, undermining and dilation and minor stress relief occurred at the toe of slope. This removal of the 'buttress' at the toe of the slope and loss of confinement may have allowed for toppling



processes to begin and migrate upslope. Movement at the toe would facilitate and provide freedom for an initial elastic response further upslope followed by brittle tensile fracturing at the base of undermined toppling pillars. Over time toppling would progress upslope and sliding would start to occur on the newly formed rough failure surface that day-lights at or near the base of the quarried rock slope. The failure surface is not a pre-existing surface in the rock mass, but rather as a result of the coalescing tensile failure surfaces (See Figure 24.). Weathering from frost and percolating water along joints may have also accelerated this process. This progressive failure would be aided (in 3D) by slippage or dilation on joints of sets J1 and J2, which – in conjunction with bedding - may ultimately be responsible for the observed tension cracks observed above the existing slide area (tension cracks observed in the same orientation as major lineaments identified during field traverses). Joints of sets J3 and J4 probably provided side release surfaces. Other pre-existing fracturing in the rock would also facilitate failure development.

In this report we refer to the “head scarp” of the 1971 slide. This feature forms a steep cliff-like face at the upslope extent of the slide which is labeled in Figure 2 as the “active rockfall zone”. The head scarp is an important feature in the analysis presented below as it forms an over-steepened section of slope where dilation can occur which may lead to upslope elastic toppling and brittle failure.

The back analysis carried out in Section 5.2 was intended to verify this tensile, but brittle failure mechanism.

4.3 Estimated Material Properties based on Field Observations

Based on limited rock characterization and testing completed by others, the joint friction angle is likely between 25-35 degrees (residual shear testing on phyllite and gouge samples reported by R&M to be 25.5 degrees, 29 degrees, 33 degrees). No cohesion was assumed for the joint shear strength.

For intact rock, possible ranges of strengths can be developed by assuming various intact rock strength values and factoring these based on different levels of damage, weathering, or degree of jointing. Geological Strength Index (GSI as provided in the program RocLab and developed by Hoek, 2002) and ‘intact’ rock strengths are provided in Table 1 and these provided a range of input parameters for the back analysis for numerical modeling. Although some discontinuities are input into the model, factoring intact strengths help account for additional discontinuities that may be present between the large scale persistent structures and small-scale incipient fracturing, since it is known that the rock mass is blocky and producing relatively uniform blocks of talus averaging about one foot in maximum dimension. The final rock strength values used in modeling were based on the back analysis of 1971 failure as described in Section 5.2 and the selected strength values used also reported in Section 5.2.



5.0 NUMERICAL ANALYSIS

5.1 Introduction

The purpose of the numerical analysis was to validate the failure mechanism envisaged for the Pillar mountain slide. The models were developed based on select cross sections cut from the LiDAR “bare earth” model as provided in Table 2.

Firstly, the back analysis of the main slide at Pillar Mountain was undertaken using the finite element program Phase2 (By RocScience), which allows for discontinuities to be inputted into the mesh domain. The back analysis is a crucial component of the modeling work since this is the primary means of calibrating the strength parameters used in the analysis of the other cross sections. The Shear Strength Reduction method (SSR) was used to identify these strength parameters. The method factors the initial strength parameters up or down until failure is initiated and the model fails to converge. For the back analysis the starting parameters were adjusted until a SSR value of less than 1 was obtained for a model run where tensile cracks were observed to coalesce (similar to the limit equilibrium Factor of Safety approach where slope stability is equal to the slope strength resistance divided by the driving forces and less than 1 indicates possible failure). Using the same calibrated starting strength parameters, the additional cross sections were analyzed and assessment was made on the stability of these slopes using the SSR approach.

The analysis was carried out using typical and elevated water tables similar that that shown in Figure 25 and bedding was assumed to dip into the face approximately 60 degrees. At the toe of slope, additional sub-vertical J1 fractures were also inputted into the model to allow for freedom and dilation near the toe of slope (or in the case of Section 4, at the crest of the head-scarp as shown in Figure 25 and Figure 26). A possible typical water table elevation was estimated based on the water table reported in R&M “Drill hole No.1 1980” (“perched” water table measurements June 14 1980 – 315’ below ground surface, September 1, 1980 – 335’ below ground surface).

5.2 Back Analysis

As described above, the back analysis at Pillar Mountain was carried out on the profile for Section 6 cut from the LiDAR terrain model and is shown in Figure 8. This profile was adjusted to reflect over steepening at the toe.

Based on the 1971 failure size, tensile crack development was expected to be some 25 feet to 50 feet below the surface, as shown in Figure 8 as a black dotted line. It is assumed that failure initiated at or near the toe of slope as the ground surface profile was over-steepened and local toppling and dilation at the toe allowed for an upslope elastic toppling response on bedding (see progressive failure development in Figures 27 to 30). The dotted black line in these 4 figures is shown only for illustrative purposes and is



based on Cross Section 4 which runs through the 1971 failure. In the modeling, however, tensile fracturing developed independent of any pre-determined failure surface but comes close as is evident when compared to Cross-Section 4 in Figure 31.

Based on the back analysis, which was completed by incrementally decreasing the strength parameters shown in Table 1 above, the following material parameters were selected as representative of the rock mass and were used in modeling the slope:

- Young's modulus = 2000 ksi (13750 MPa)
- Joint Friction Angle = 33 degrees (joints – bedding and local J1 jointing in toe area)
- Joint Cohesion = 0 (joints)
- Rock mass Tensile strength = 130 psi (0.9 MPa)
- Rock mass peak frictional angle = 37.6 degrees, residual = 31.5 degrees
- Rock mass peak cohesion = 230 psi (1.6 MPa), residual = 130 psi (0.9 MPa)

The back analysis using these parameters indicates that the SSR of the Pillar Mountain slide is less than 1, for the failure volume shown in Figure 32. This indicates that the assumed strength parameters for the joint sets and continuum are fairly well calibrated and can be used in the validations of the failure mechanism and stability checks for the slide area in its current configuration. The model failure zone is indicated in the figure by calculated but not calibrated displacements which are presented as colors. This colored zone is used in this figure only to show the zone on the slope where movement was calculated above the tensile failure plane indicated in Figure 31.

5.3 Shallow and Global Failure Analysis

5.3.1 Shallow Failure Analysis

After the back analysis was complete, the calibrated material properties were used to analyze the stability of Cross-Sections 4 and 1. We have assumed that the joint sets present in the 1971 failure are ubiquitously developed throughout the rock mass and therefore the same geological conditions are present at the existing head scarp (Section 4) and in the adjacent, but more benign slopes (Section 1). Since the relevant joint sets are the same, and are favorable, it is interpreted that failure can only occur if intact rock fails, as described for the back analysis.

Section 4 comprises an over-steepened section of slope, at the main head-scarp as a result of the 1971 failure. Field observations indicate that some dilation and rockfall is ongoing at the crest of the head scarp. The progressive nature of tensile fracture development for the head scarp area in Cross Section 4 is shown in Figures 33 to 37 and the size of failure is approximated by the deformation contours shown in Figure 38.



SSR iterations were run for the models produced for Section 1 and Section 4 in order to simulate three scenarios – 1) typical water table, 2) an elevated water table, and a typical water table with a seismic Kh coefficient of 0.2g. The results for these simulations are described in more detail in Section 5.3.3.

5.3.2 Global/Deep Seated Analysis

Additional SSR iterations were run to try to assess the required reduction in rock strength parameters over and above that required for the smaller-scale shallow failure mechanism described in Section 5.3.1. While the analysis procedure used for the shallow analysis described above and that used for global/deep seated analysis is almost identical, the results are very illuminating because it becomes apparent that the failure mechanisms that govern global failure are very different than those present during shallow-type failures.

In order for the deep-seated failure to occur (See Figures 39 and 40.), shear fracturing would need to develop through the confined rock mass for a failure plane to develop. The modeling shows that the strength parameters would need to be reduced by a factor of at least 1.5 compared to the initial properties assumed from the back analysis and an elevated water table would need to be present for this type of failure to be feasible. This process was completed for both Section 1 and Section 4 for the elevated water table, the typical water table, and the typical water table with a 0.2g seismic Kh coefficient applied in the horizontal direction.

It is evident from Figures 39 and 40 that the size of failure is much larger and that failure initiates by crushing of rock at the toe of slope, extending upward in a circular-type failure mode. Shear fracturing is indicated by the red “x’s” in Figure 39 and the overall global failure magnitude is provided in Figure 40.

Results for these simulations are described in more detail in in Section 5.3.3.

5.3.3 Results Summary (Shallow and Deep Seated Failure)

The modeling carried out for the slope at Pillar Mountain was intended to validate the envisaged shallow toppling failure mechanism and also assess the global failure potential and mechanism. The Shear Strength Reduction method (SSR) was used to reduce the parameters used in the back analysis for each of the cross sections analyzed so the stability of each cross section could be compared in a relative sense. For comparative purposes, the ranges of SSR values where tensile cracks coalesce are presented in Table 3, however, the relative risk of each failure mode is described in more detail in Section 5.1.

It should be noted that in all our analyses the impact of seismic events were assessed using a Kh = 0.2g which is considered by Terzaghi (1950) to be in the “violent and destructive” category of shaking. We understand that the peak ground acceleration is 0.4g for the 1 in 500 year seismic event at the site and



modeling was run using a pseudo static -type analysis that considers half the PGA and is applied horizontally. This is considered to be reasonable because the model does not consider the time history and duration of shaking and it is unlikely that 0.4g occurs throughout a seismic event. The seismic SSR estimates shown in Table 3 should only be viewed as indicative, since the PGA in itself has limited application in seismic slope stability-type assessments. The results showed that the potential for global shear-induced failure is $1 < SSR < 1.3$. These estimates should only be viewed as indicative, since a single acceleration value, as assumed in pseudo-static analysis, in itself has limited application in seismic slope stability assessment.



6.0 DISCUSSION AND CONCLUSIONS FROM SITE RECONNAISSANCE AND MODELING

6.1 Relative Probability of Failure

The conclusions drawn for field observations, reports by others, and modeling are that the structural geology of the site is generally favorable from a stability perspective and therefore translational or circular sliding on a discrete weak surface is not occurring in this locality. It is also contended that the 1971 failure was primarily precipitated by quarrying activities at the toe of slope, which over-steepened this area of the slide. This over-steepening probably facilitated rock mass movement upslope (but to a limited depth) with toppling and tensile fracturing perpendicular to bedding as described more fully in Section 4.2. It is also concluded that this type of failure mechanism is limited to the remaining over-steepened areas of the slope (head scarp of 1971 slide in particular) and failure of this nature will only occur to a limited depth and size. It is also concluded that global failure of the mountain in this vicinity is unlikely.

The numerical modeling carried out using Phase2 was able to demonstrate that the mechanism described in Section 4.2 is valid for shallow failures and likely contributed to the 1971 event at Pillar Mountain. It is, however, not known if displacement and rock damage occurred during historic large seismic events and if this contributed to the 1971 failure. Although unlikely, it is also not known if deep-seated, unfavorably orientated faults or weak features exist at depth below the slide. If such features exist, then the global failure mechanism described herein may need to be reconsidered. Additional drilling and downhole borehole camera work would likely be required to investigate this further, but is not considered necessary at this stage.

Based on the distribution of the SSR values obtained in the analysis, and summarized in Table 3, and considering all other information available, it is our considered opinion that on a relative scale we can conclude the following (to be read in conjunction with Table 4):

- There is a very low probability of a global deep-seated failure in the vicinity of the Pillar Slide. It would require an extreme set of circumstance or unforeseen condition to be present for this to occur. This is discussed further below.
- There is very low probability of the existing slopes adjacent to the slide area failing in a similar fashion to the 1971 failure. Adjacent in this case refers to slopes not affected by actual 1971 side area itself. This is discussed further below.
- There is moderately high probability of the existing head scarp failing further up-slope (over-steeped section of the 1971 slide compared to the rest of the slope). This will likely be a relatively shallow failure and will likely be progressive in nature.
- There is a moderate to high probability that rockfall will continue from the head scarp area of the 1971 slide (limited volume of material – similar to that occurring at present).



6.2 Progressive Nature of Failure and Importance to Future Instability Predictions

It was described in the R&M report that the initial failure began on December 5, 1971 when large amounts of rock debris began falling from a “vertical gully” feature in the exposed bedrock. The failure progressively raveled over the next four days from an elevation of 300 feet to approximately 775 feet a.s.l. Fractures (interpreted as tension cracks) continued to open up to elevation 1125 feet a.s.l. during a heavy rainfall period up to December 17, 1971 and rock fall was continually reported throughout this period. The R&M report noted that the activity of the Pillar Mountain Slide has remained low in the years following 1971 and this has been confirmed by the previous two site visits made by Golder.

Based on the observations made during the 1971 failure and the forward analysis completed using Phase2, it is anticipated that future activity at Pillar Mountain will occur in a similar progressive fashion. It is anticipated that under elevated pore water pressure conditions, progressive tensile fracturing and damage of the rock mass will be ongoing and result in progressive sliding if these conditions are sustained. The exact size and magnitude are difficult to predict as tensile fracture formation will be in part related to the location of pre-existing fractures and discontinuities in the head-scarp. For this reason, it would be very beneficial to monitor displacements of the mountain to assess the magnitude (both movement magnitude and areal extent) and direction of movement in this area, and the mountain as a whole. In the future, this data could be used in to determine if mitigation measures are required beyond the gabion wall present at the base of the slope and would, as a byproduct, also help with more sophisticated models to assess strain softening properties and calibrate to the measured displacement, which was not feasible for this assessment. Furthermore, monitoring would help identify whether slope accelerations are occurring and help identify the risk of both moderate-size and global-scale failure.

6.3 Stability of the Upper Head Scarp

Depending on the season and the amount of rainfall, it is considered possible that an elevated, but transient, water table can exist in the mountain. As a result, small but progressive deformation of the upper head scarp area above the 1971 slide area may be ongoing as evidenced by continuing but small rockfall events. The SSR or Factor of Safety of these upper slopes is likely close to 1 under elevated groundwater conditions. However, under more typical groundwater conditions (i.e. the water table is below the base of the head scarp) modeling and back analysis indicates that the Factor of Safety is likely higher and movement may be related to local frost jacking, and weathering, which can also produce small-scale rockfalls.

Furthermore, modeling suggests that it is highly likely that the tension cracks or lineaments observed upslope from the existing failure are a consequence of ongoing toppling as well.



6.4 Seismic Considerations

It is expected that significant damage will occur to the upper head-scarp during a large seismic event and this will result in rockfall and possible failure similar to that shown in Figure 38. In addition, for sustained horizontal ground motions exceeding 0.2g it is possible that a larger scale failure (such as the global scale failure previously outlined by R&M) could be activated, however, the amount of deformation will depend on the duration and nature (time history of acceleration) of the shaking at and above the predicted PGA and other factors such as pore water pressure buildup in the rock mass at the time of failure.

6.5 Stability of Flatter Slopes Adjacent to 1971 Failure

The slopes adjacent to the main failure scarp (such as shown in Section 1 – Figure 8) have a flatter overall slope angle and do not have over-steepened slope sections. Apart from minor toe dilation, the failure mechanism described at length above was not observed in modeling for Section 1. This confirms that the shallow failure mechanism is likely not feasible for slopes outside the 1971 slide area.

Most of the slope is flatter than the area associated with the 1971 slide, and this combined with the assumption that the typical water table is likely some 300 feet (measured vertical as indicated by the R&M borehole) below the ground surface provided credence that the slope is generally stable away from the 1971 slide area. There is the potential that fluctuations in water table and pore water pressure buildup in joints during heavy rainfall will lead to ongoing tensile failure in the rock mass, but this effect is transient.

6.6 Global Failure

Modeling has demonstrated that in order for a deep-seated failure to occur it requires a reduction in material strength properties assumed in the back analysis of the previous 1971 failure by a factor of at least 1.5. The rock mass is also required to have elevated pore pressures to induce failure. Nothing we have done or seen indicates that a deep-seated global failure has ever occurred at this site or will ever occur. The 1971 slide was large, but not deep-seated and it took almost a month to complete its periodic dumps of talus down the slope.

As noted above our analyses show that in addition to over steepening the face of this slope, significant rises in pore water pressure would be necessary to cause a deep-seated global slide. This can occur during periods of heavy rain. It can also occur when subsurface water flow is dammed by something else, for example a hard freeze which would seal the active layer with frost. In Kodiak it rains frequently but not the total rainfall is low. In 1971 just before that slide, which was not deep-seated, the rainfall totals had been low. There was a heavy freeze, night time temperatures were around 0 degrees Fahrenheit for a week or more, as shown in Figure 3. Our model studies indicate that the prime cause of the initiation of the slide was likely the over-steepening of the slope by the quarrying at the toe of the slope. The analyses show that the magnitude and length of the sliding that actually occurred in 1971 likely needed for the pore pressures at the time to be higher than those measured in the 1982 investigation. An



unusually cold period of freezing could have been a major contributor to the increased size and activity of the 1971 slide by causing the pore pressures to be higher at that time.

In the modeling, the rock mass strength parameters used at depth are the same as the strength parameters used in the model near the surface. The exception to this is that bedding was not added at depth to simplify the modeling process. This is considered to be reasonable because with increased depth below surface, confined rock mass conditions are likely to improve and this factor will play a significant role, but it is difficult to explicitly include this in the modeling without more data. Based on the historic R&M boreholes it was observed that the rock quality did in fact improve with depth, and for this reason the strength parameters used in the modeling are likely conservative for the global failure mechanism.

In a relative sense the modeling has also shown that even with the use of the same material properties at depth as determined in the back analysis, topple-type movement with tensile failure through beds, as seen in the upper head-scarp and over-steepened sections of the slope, is not a likely mechanism for deep-seated global failure. The failure mechanism ascribed to the 1971 failure, and possible progressive failure of the same slide area upslope, is considered not to be possible on the global scale of the mountain for reasons described above. The modeling confirms this, i.e., shearing through the rock mass would need to occur, and this is unlikely since the rock mass condition at depth are unlikely to be worse than those encountered at surface.



7.0 SUMMARY OF CONCLUSIONS

The following are a summary of the conclusions that have been discussed in more detail in previous sections of this report:

- Rockfall will continue on this slope for the foreseeable future.
- Most of the rockfall (talus) will consist of relatively uniform blocks about the size of the talus currently on the slope.
- The current gabion walls need maintenance including the following:
 - Removal of some of the talus that has piled up behind it.
 - Repair of the damaged baskets.
 - Increase the height of the walls to reduce the chance for rockfall on the highway.
- Monitoring any rockfall would help predict future problems.
 - Notations of the time and volume of rockfalls could aid in future evaluations
 - Notations of rockfall damage could aid future evaluation
- The LiDAR base data obtained may provide a base for slope movement measurements.
- An early hard freeze may have contributed to the 1971 slide.
- There have been no indications found of a deep-seated global slide at this site
- Our analyses show that a deep-seated slide is unlikely unless:
 - There are very unusual climatic conditions
 - There is a very large earthquake with large ground motions close to the site
 - There is additional excavation activity on the slope.



8.0 RECOMMENDATIONS

As has been discussed above, this slope will continue to produce rockfall. The existing gabion barrier is retaining most of the rock that could reach the highway or the docks below. Any additional stabilization of this slope would be very expensive and may not be necessary as long as the continuing rockfall volumes are acceptable. Therefore, we have developed recommendations that would improve the status quo and may give you early warning if there is a large slide about to occur. Our recommendations are as follows:

- Maintain the current gabion walls including the following:
 - Remove of some of the talus that has piled up behind it. This should be done under the supervision of an engineer familiar with rockfall risks.
 - Repair the damaged gabion baskets.
 - Increase the height of the gabion walls to reduce the chance for rockfall on the highway. This should be done under the supervision of an engineer familiar with rockfall risks.
- Monitor the slope by:
 - Documenting significant rockfall events with pictures and written notes
 - Large rockfalls
 - Talus reaching near the top of the gabion walls
 - Rocks or rock damage occurring on the highway or guard rails.
 - Cracking of or damage to the highway pavement in the slide zone
 - Rerunning the LiDAR data acquisition to determine if useful ground movement information can be obtained.
 - After a large slide
 - After a large earthquake
 - Every two to four years if meaningful data is being obtained.

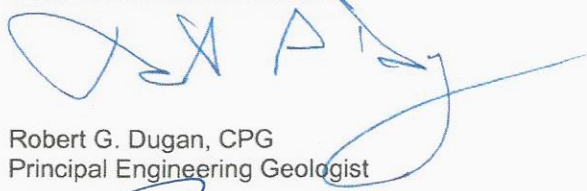


9.0 CLOSURE

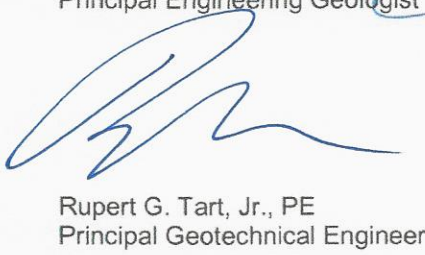
This report is the product of several key people and organizations. The project management and review, graphics and imagery analyses, and site reconnaissance were done by our Anchorage staff members including Bucky Tart, Bob Dugan, Howard Weston, and Andy Garrigus. The numerical modeling and rock mechanics analyses were done by Paul Schlotfeldt and Brad Panton of Golder's Squamish, BC office. The LiDAR was acquired and processed for our use by Kodiak Mapping Inc. under the direction of Jeremy Smith.

Thank you for the opportunity to review this very interesting rock slide and prepare this report. Please contact us if you have any questions.

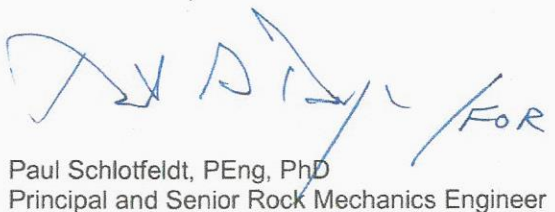
GOLDER ASSOCIATES INC.



Robert G. Dugan, CPG
Principal Engineering Geologist



Rupert G. Tart, Jr., PE
Principal Geotechnical Engineer



Paul Schlotfeldt, PEng, PhD
Principal and Senior Rock Mechanics Engineer



RGD/RGT/PS/mlp





10.0 REFERENCES

Golder Associates Inc., November 14, 2002, Report- Pillar Mountain Slide Reconnaissance, prepared for the City of Kodiak.

R&M Consultants, 1982, July 1982, Pillar Mountain Slope Stability Study, Final Project Report, prepared for the City of Kodiak.

Kachadoorian and Slater, 1978, Pillar Mountain Landslide, Kodiak, Alaska, U.S. Geological Survey Open File Report 78-217

Terzaghi K. "Mechanisms of Landslides." Engineering Geology (Berkeley) Volume, Geological Society of America, 1950.

Kodiak Mapping Inc., 2013, LiDAR Survey.

<http://www.rocscience.com/products/3>

TABLES

Table 1

Ranges of Assumed Factored Rock Mass Strengths Values for Back Analyses

Unconfined Compressive Strength (psi)	GSI	Tensile Strength (psi)	Equivalent Mohr Coulomb Properties	
			Friction Angle	Cohesion (psi)
3600 (25 MPa)	100	500 (3.5 MPa)	47 (low normal stress)	750 (low normal stress)
3600	100	500	40 degrees	770 (5.3 MPa)
3600	90	250	40 degrees	450
2900 (20 MPa)	90	190	39 degrees	360
3600	80	120	39 degrees	280
2900	80	90	37 degrees	230
3600	70	55 (0.37 MPa)	37 degrees	190 (1.3 MPa)

Table 2

A Summary of Analysis Types and Cross Sections Used (see Figure 7 for location of cross-sections and Figure 8 for the profiles along the cross sections.)

<u>Analysis</u>	<u>Cross Section</u>	<u>Analysis Description</u>
Back Analysis	6	<i>The back analysis was used to calibrate the strength parameters for use in the shallow failure and global failure analysis. Cross Section 6 is assumed to be very similar to the pre-failure ground surface prior to the 1971 slide. This slope profile was subsequently over-steepened in the toe area to reflect quarrying in the toe area of the slope – described in detail in Section 5.2.</i>
Shallow Failure Mechanism Analysis	4	<i>Cross section 4 was cut through the main Head scarp of the 1971 slide. Numerical models were run using the parameters calibrated from the back analysis. Three model iterations were run including an assumed elevated water table, a typical water table, and the typical water table with a seismic loading coefficient of 0.2 – described in detail in Section 5.3.</i>
Global Failure Mechanism Analysis	4	<i>Further to the shallow failure analysis for Section 4 the global failure mechanism was also assessed using the same section.</i>
Shallow Failure Mechanism Analysis	1	<i>Cross Section 1 was cut through the more benign slope to the east of the 1971 slide area. The same methodologies and model iterations used for Cross section 4 were applied.</i>
Global Failure Mechanism Analysis	1	<i>Further to the shallow failure analysis for Section 1 the global failure mechanism was also assessed.</i>

Table 3

Shear Strength Reduction Method Results Summary for Various Analyses

<u>SSR Range at Failure</u>	<u>Analysis for Each SSR Range</u>
SSR<1	- Back analysis (saturated), failure of slope occurred as a result of quarrying at toe and elevated pore pressures.
1<SSR<1.3	- Shallow Failure Main Head scarp Section 4 (elevated WT) - Global Failure Section 4 with seismic Kh = 0.2g*
1.3<SSR<1.5	- Shallow Failure Main Head scarp Section 4 (typical WT) - Global Failure Section 1 for seismic Kh =0.2g*
SSR>1.5	- Shallow Failure for Section 1 is not feasible since the cross section does not contain over-steepened or unconfined slope sections. - Global Failure Section 4 (both water tables) - Global Failure Section 1 (both water tables)

*Pseudo static analysis considered Kh = 0.2g, typical water table assumed for this analysis.

Table 4

Relative Risk Comparison for Various Failure Modes at Pillar Mountain

<u>Failure Type</u>	<u>Relative Probability of Occurrence</u>
Minor Rockfalls Originating from the Head Scarp	High – rockfalls up to several 100 cubic feet are expected to continue to initiate from the upper head scarp
Failure of Upper Head Scarp and Over Steepened Slope Sections (topple induced brittle/tensile failure – magnitude shown conceptually in Figure 38)	Moderate – progressive deformation and failure is possible in local areas of the upper head scarp and for over steepened slope sections.
Global Failure of Pillar Mountain (shearing required perpendicular to bedding – magnitude shown conceptually in Figure 40)	Low – shear failure through confined intact rock is unlikely and there is no explicit evidence that there is a deep-seated, unfavorably orientated fault or feature that would be contributing to global failure of Pillar Mountain. Under seismic loading, activation of a global scale failure is more likely but is dependent on the magnitude and duration of shaking and the pore water pressure present in the mountain at the time of an earthquake event.

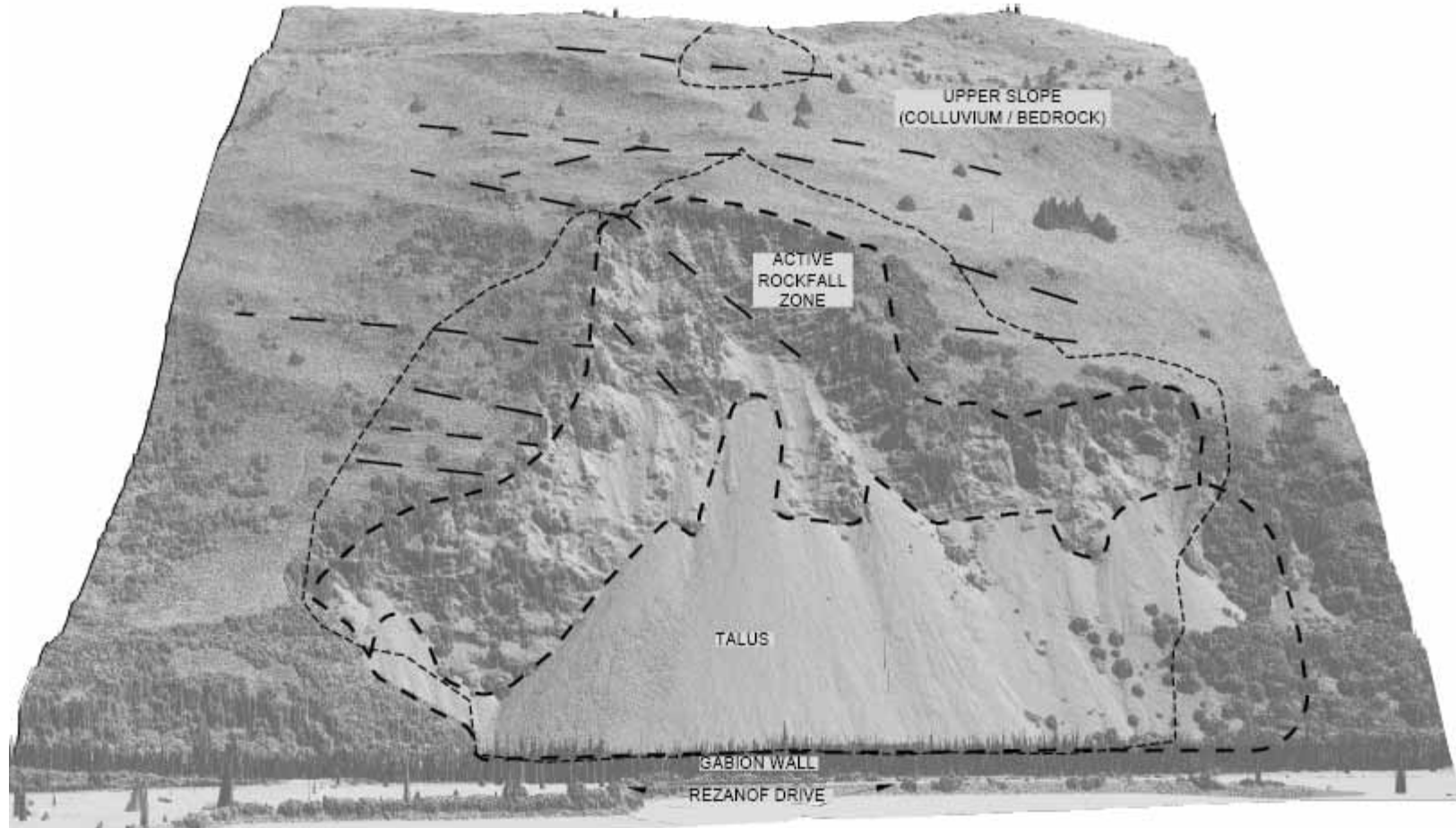
FIGURES



Vertical Colorized LiDAR Image of Pillar Mountain Slide

Figure 1

Project No.1300823



LEGEND

- APPROXIMATE LOCATION OF GEOLOGIC CONTACT
- - - APPROXIMATE LOCATION OF LINEAMENT
- APPROXIMATE LOCATION OF RECONNAISSANCE ROUTE

REFERENCE

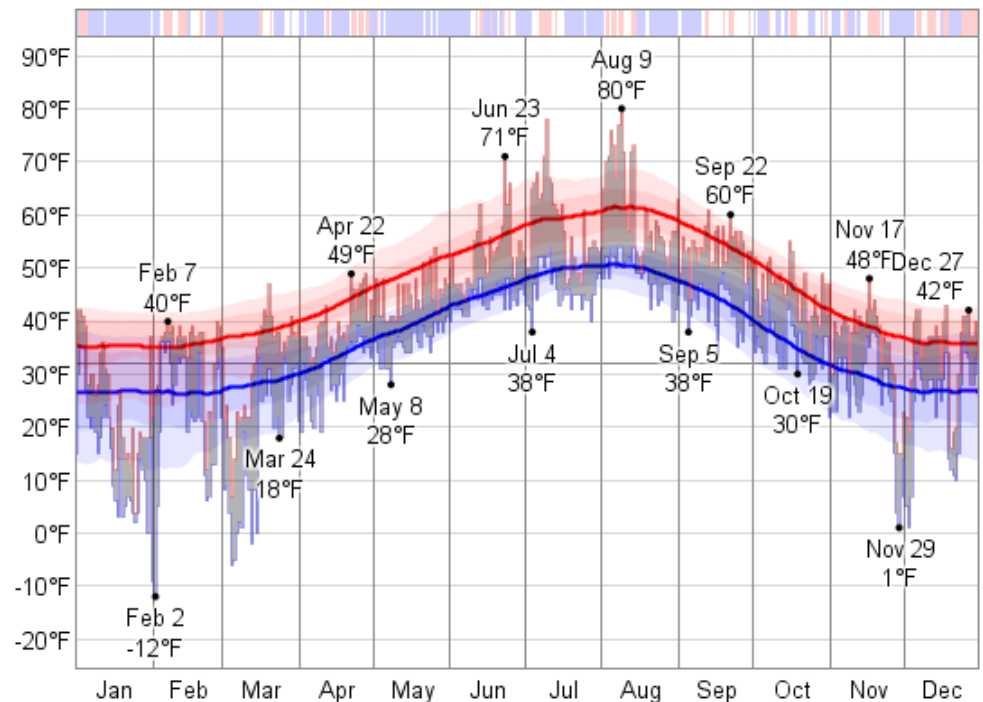
HILLSHADE GENERATED FROM LIDAR POINT CLOUD
 COLLECTED BY KODIAK MAPPING AND DELIVERED ON
 8-28-2013.



Oblique Bare Earth View of Slide Area
 Using Hillshade from LiDAR Data

Figure 2
 Project No.1300823

Temperature



The daily low (blue) and high (red) temperature during 1971 with the area between them shaded gray and superimposed over the corresponding averages (thick lines), and with percentile bands (inner band from 25th to 75th percentile, outer band from 10th to 90th percentile). The bar at the top of the graph is red where both the daily high and low are above average, blue where they are both below average, and white otherwise.

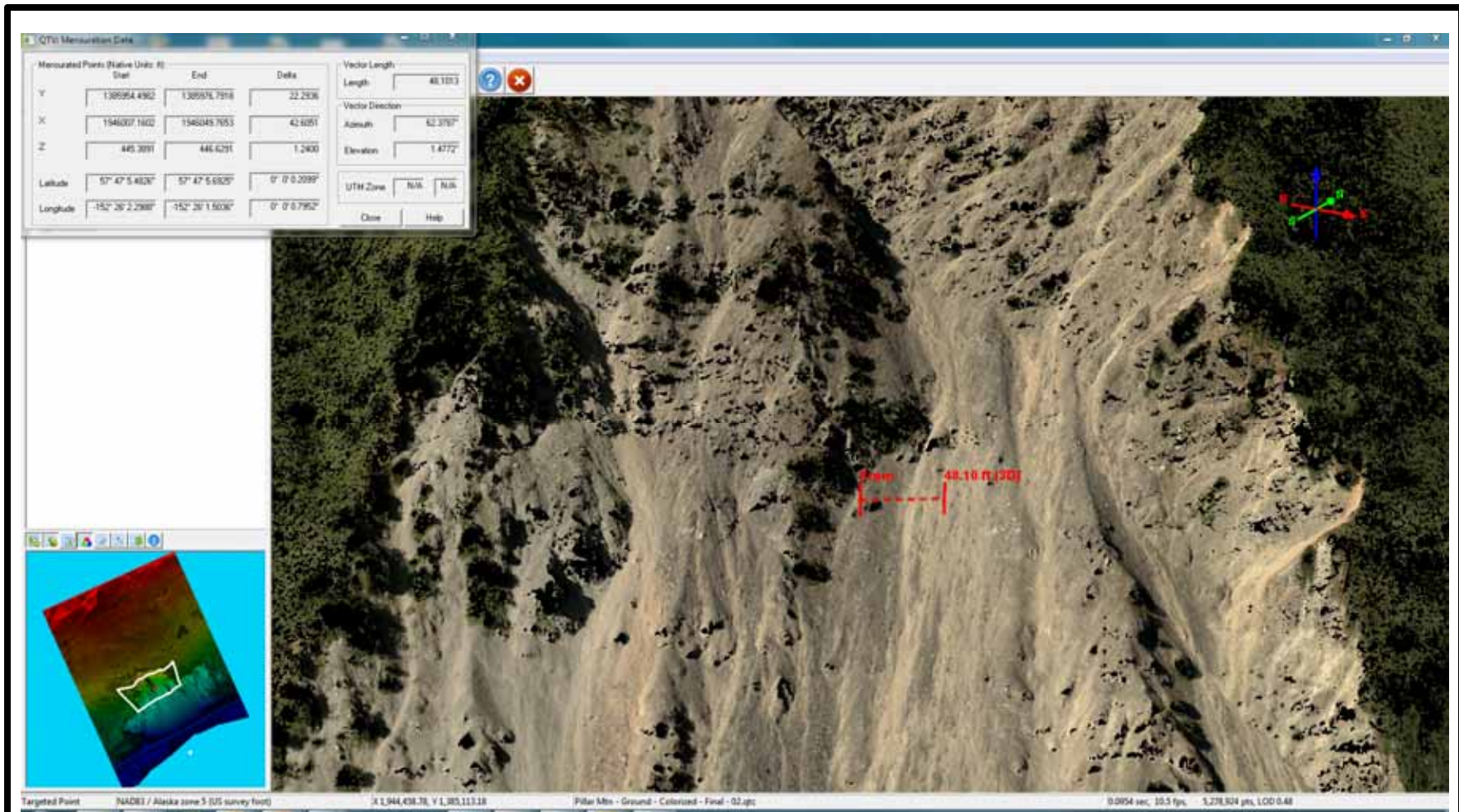
<http://weatherspark.com/history/32927/1971/Kodiak-Alaska-United-States>



Kodiak Air Temperatures in 1971

Figure 3
Project No.1300823





Ground Distance Measurement on LiDAR Model

Figure 5
Project No.1300823



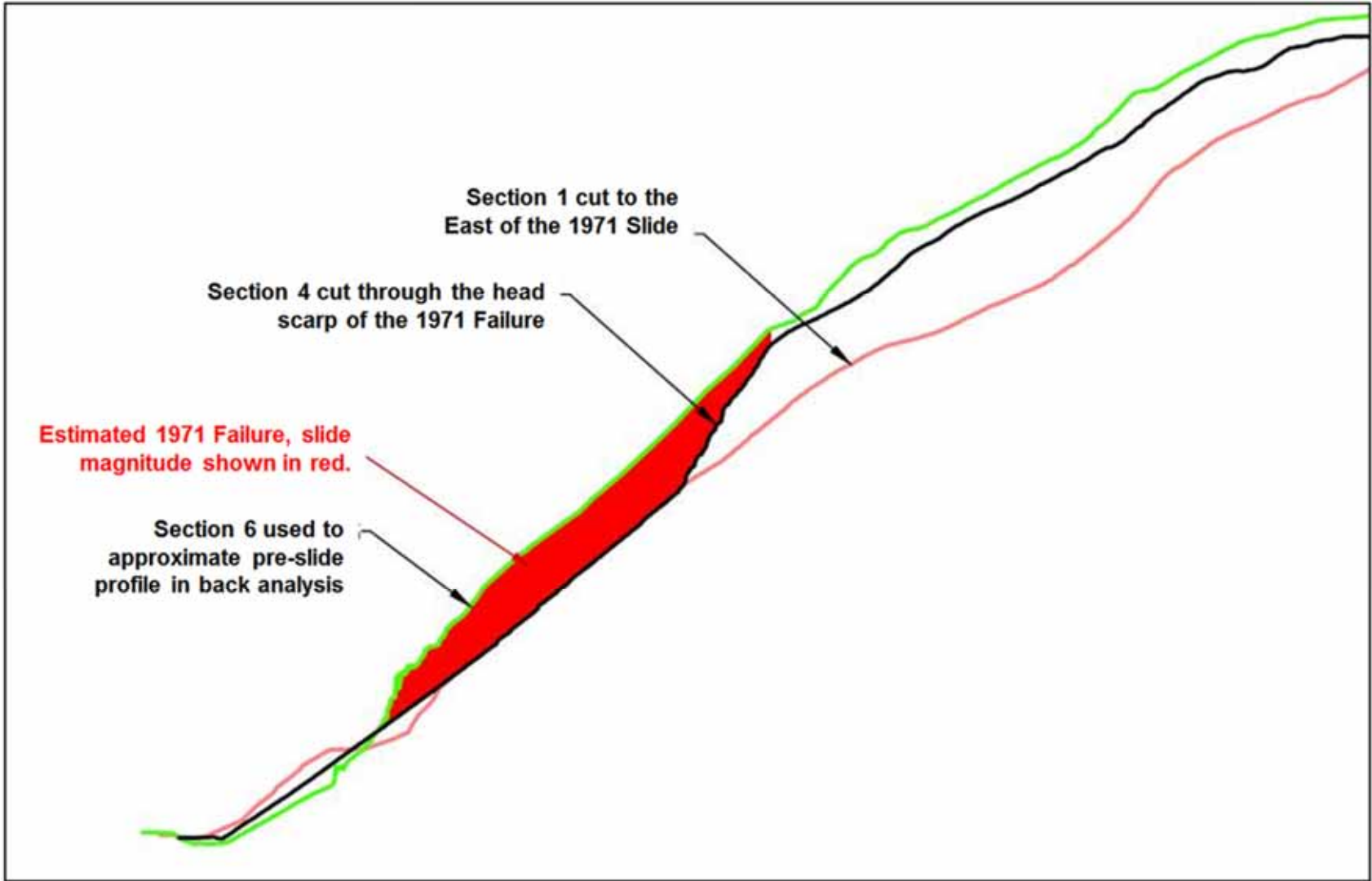
Area Covered Targeted in LiDAR Survey

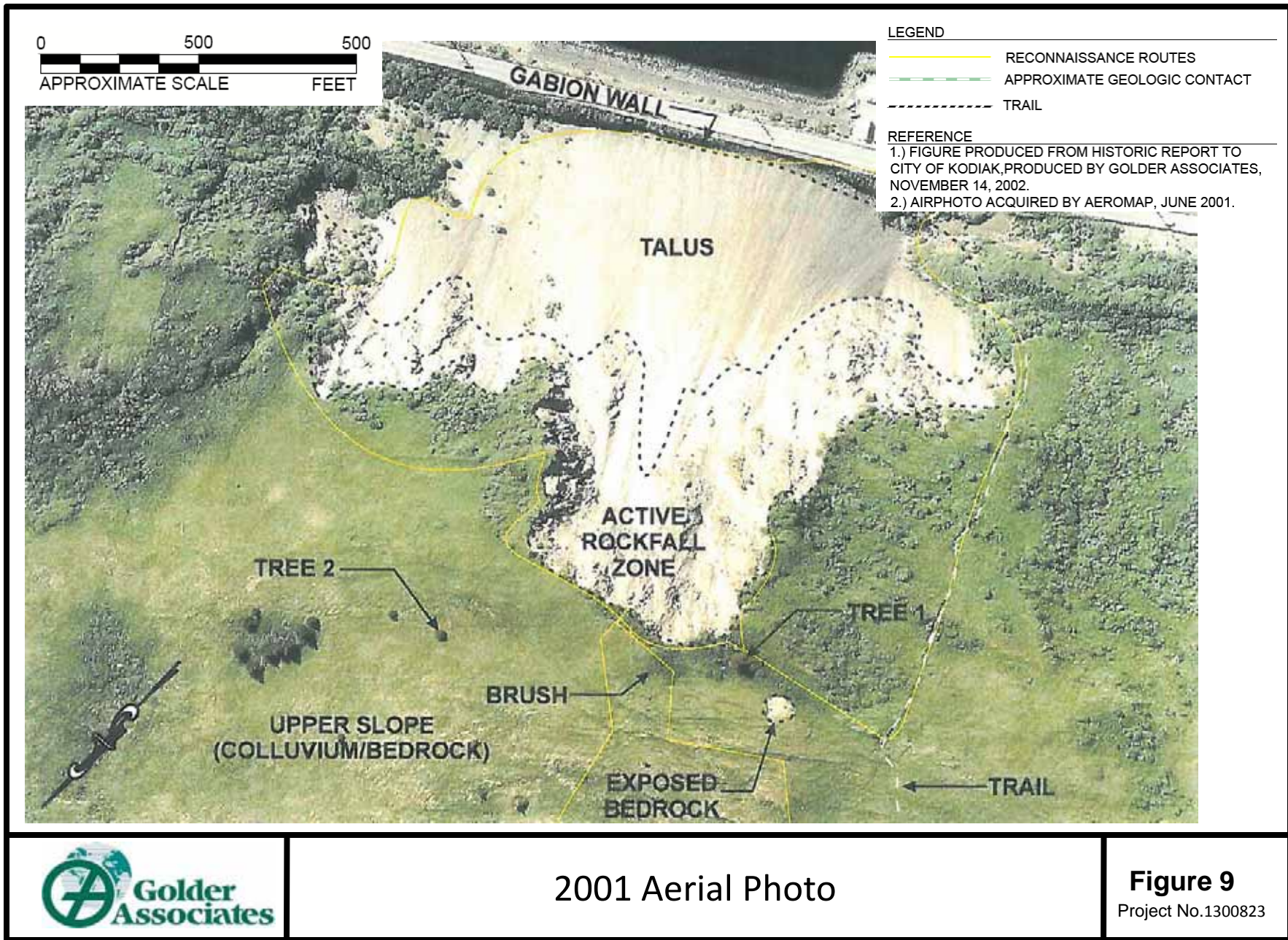
Figure 6
Project No.1300823



Three Cross Sections Selected for Numerical Analyses

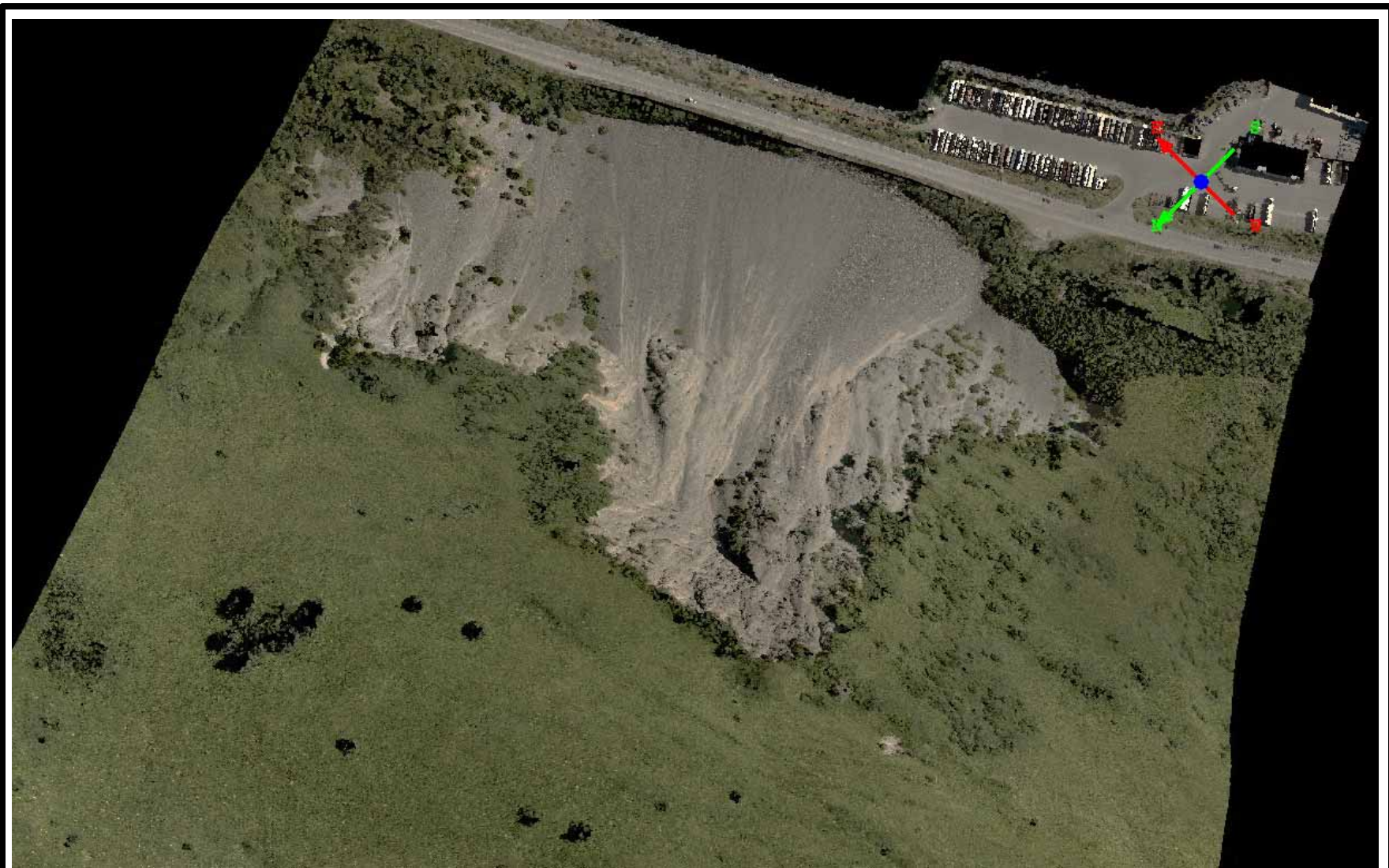
Figure 7
Project No.1300823





2001 Aerial Photo

Figure 9
Project No.1300823



2013 LiDAR Image of the Slide

Figure 10
Project No.1300823





View Downslope from Head-scarp
(September 21, 2013)

Figure 12
Project No.1300823



View of Northeast Side of Slide Area
(September 21, 2013)

Figure 13
Project No.1300823



Toe of Talus Cone with Gabion Wall to the Left
(September 21, 2013)

Figure 14
Project No.1300823



View of Upper Slope Terrain Above the Head Scarp
(September 21, 2013)

Figure 15
Project No.1300823





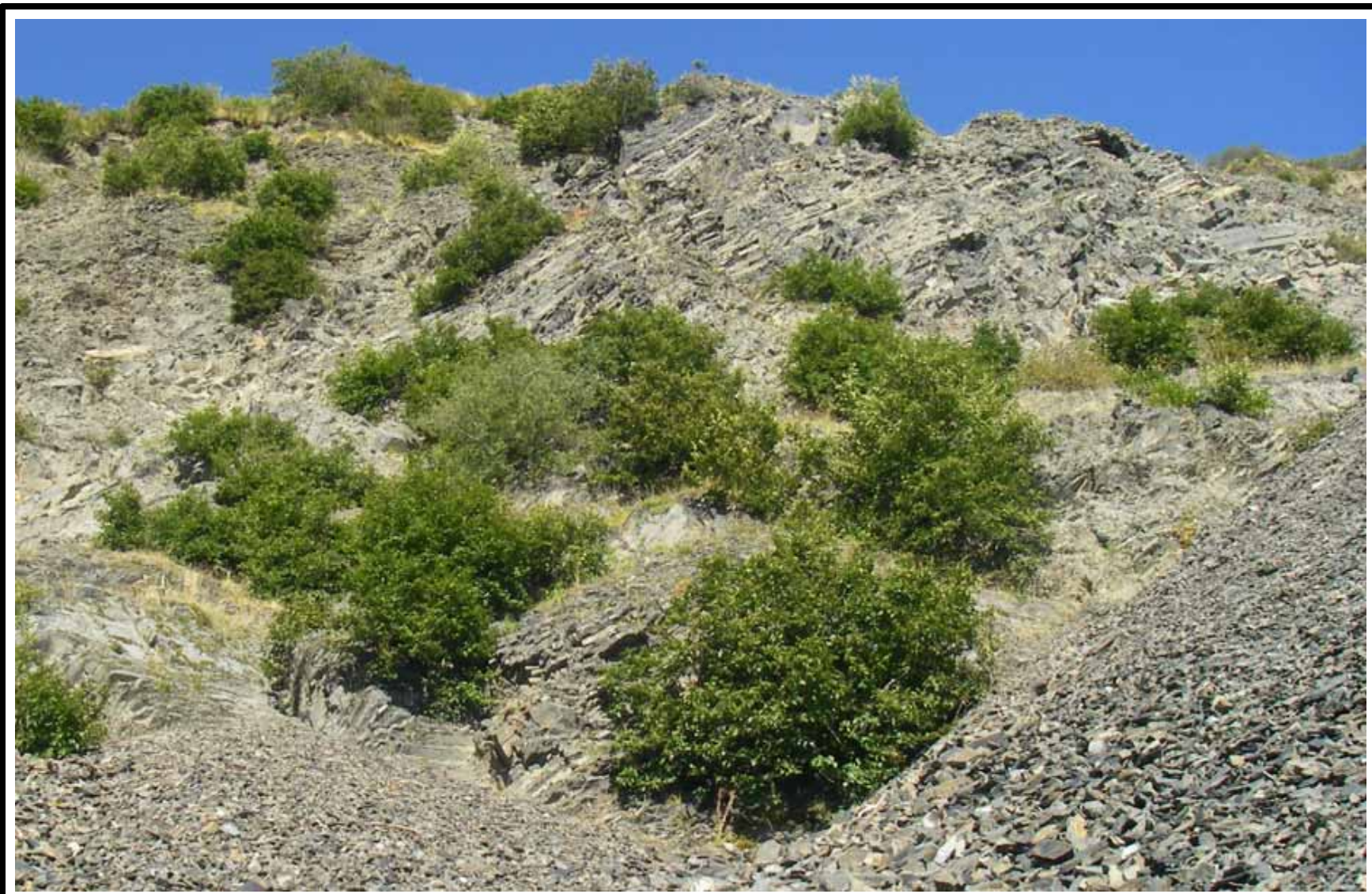
Rockfall across Road and Impact Craters on Pavement
(September 21, 2013)

Figure 17
Project No.1300823



Larger Rocks Retained by Gabion Wall

Figure 18
Project No.1300823



Typical Head Scarp Rock Structure

Figure 19
Project No.1300823



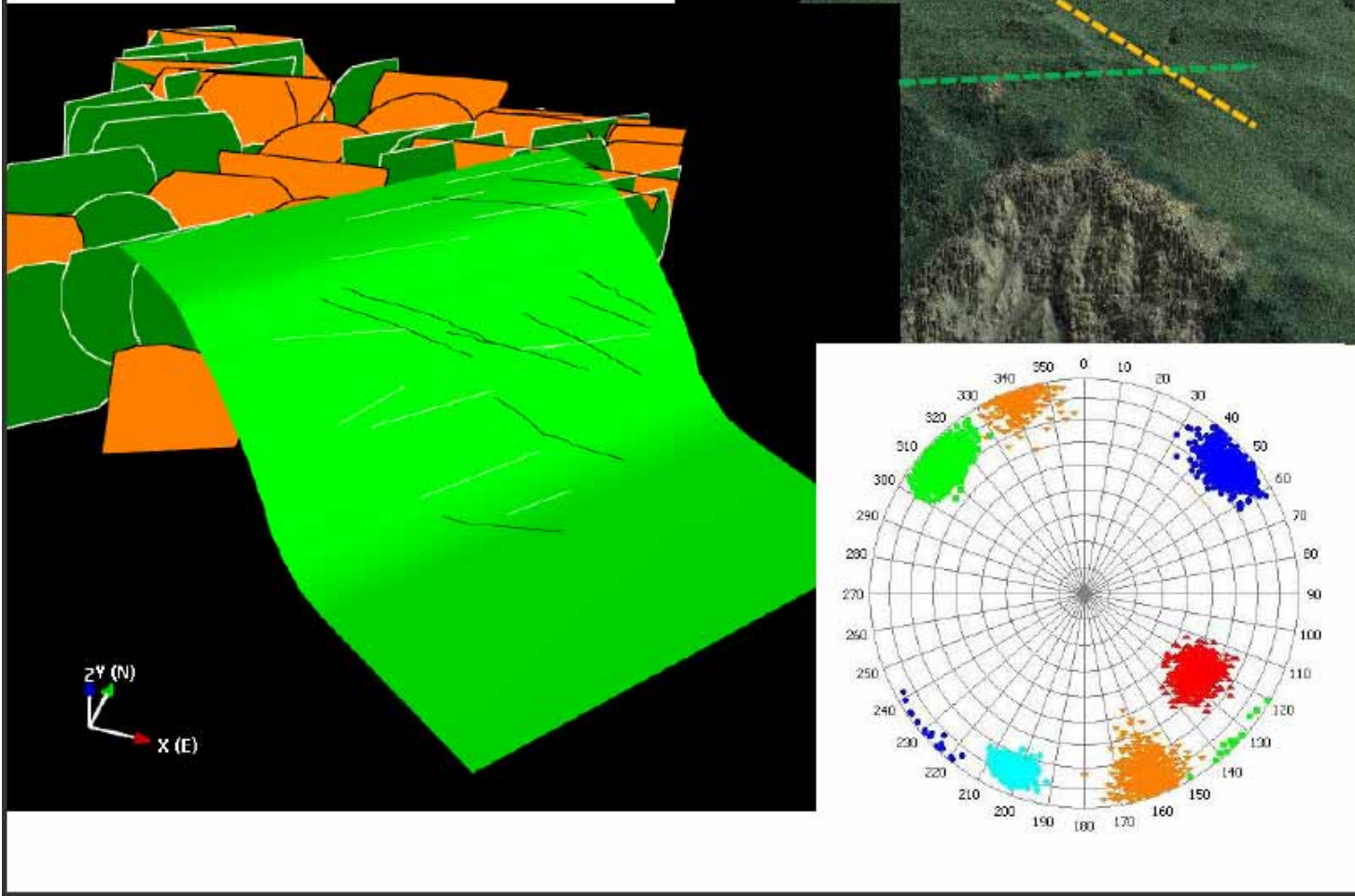


Cross Slope View of Head Scarp Rock Structure

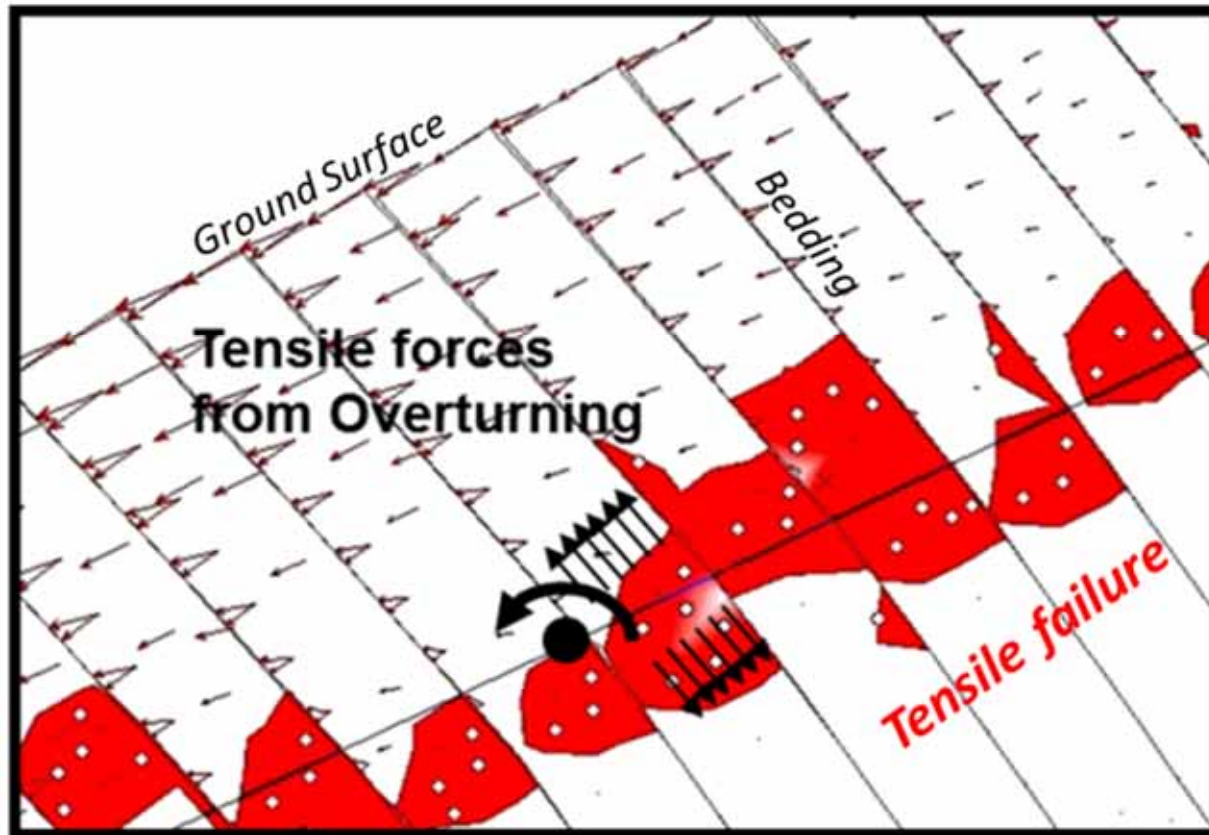
Figure 21
Project No.1300823

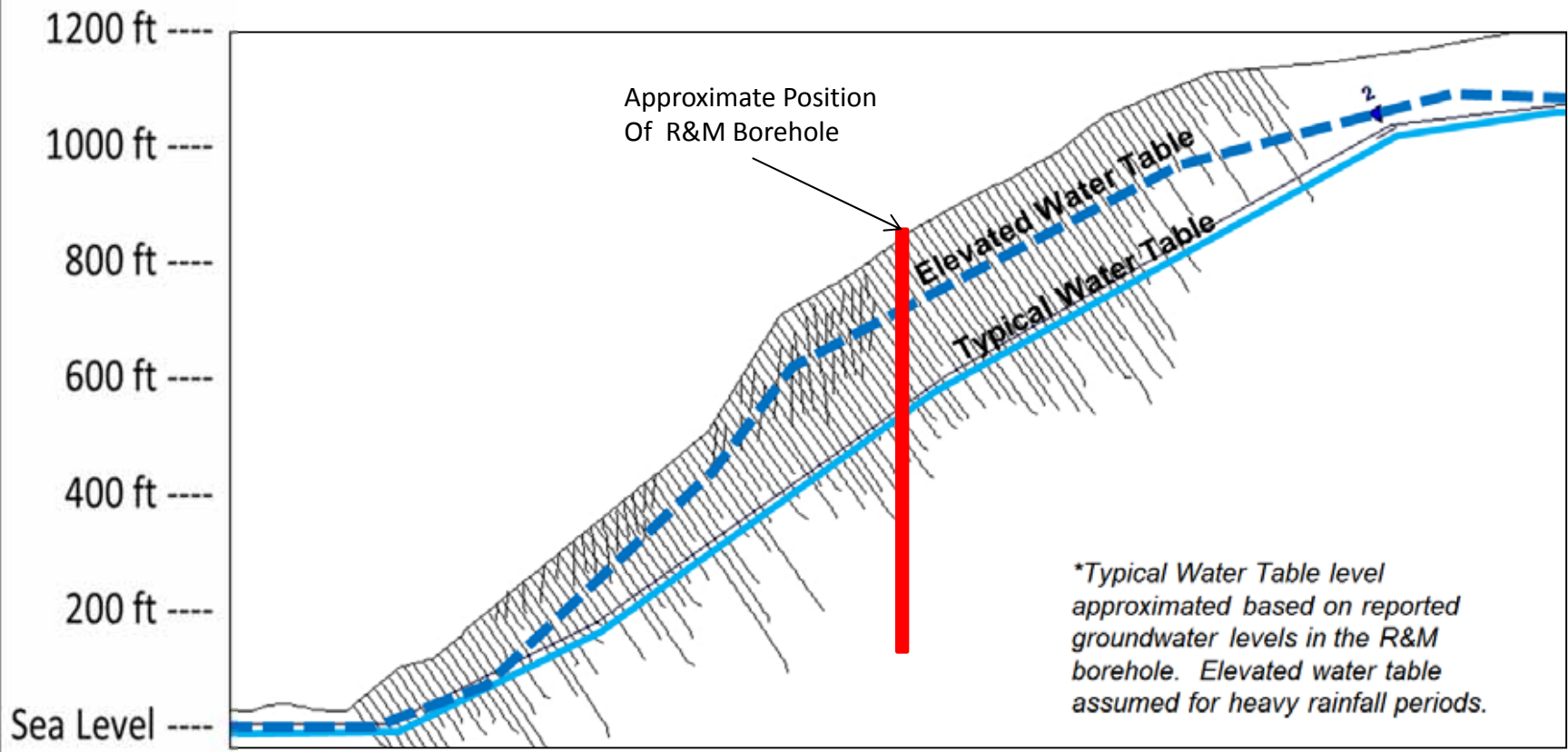


J1 and J2 – Back Release Surfaces
(possible lineaments)



Failure in tension indicated by red 'o'
(governed by tensile strength of rock mass)



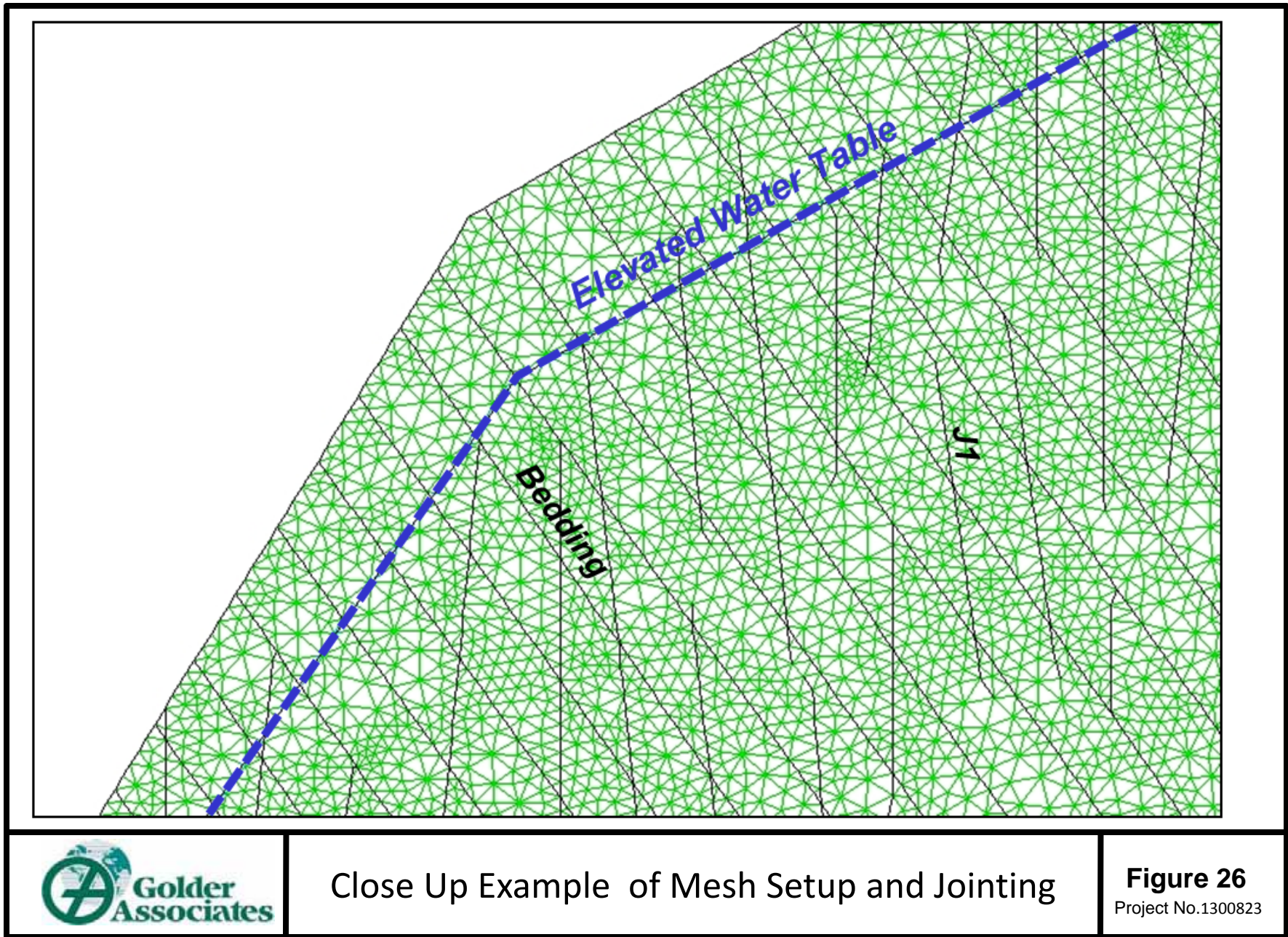


Note: Elevations and dimensions implied are approximate

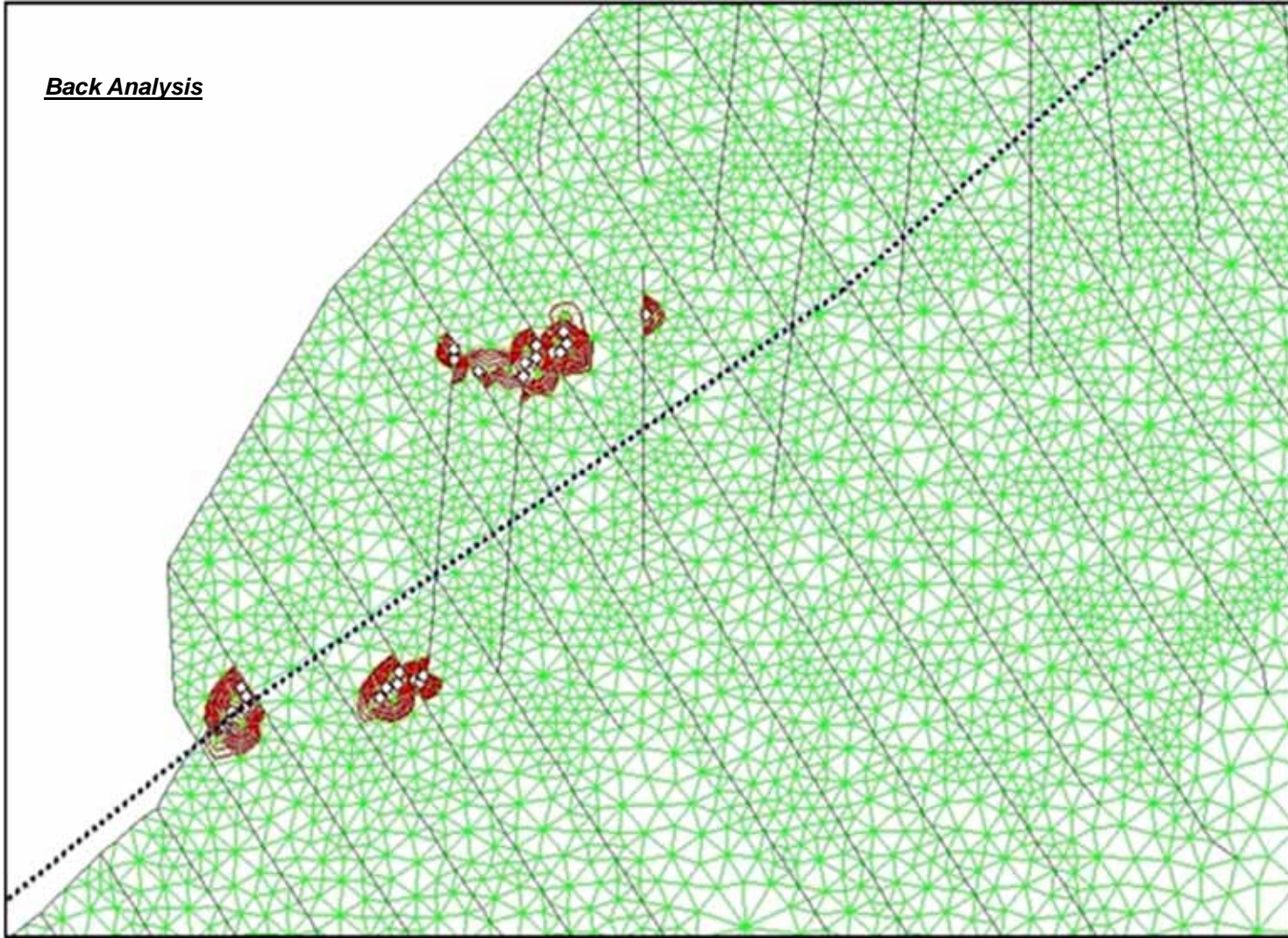


Example of Typical and Elevated Water Tables Shown for Section 4

Figure 25
Project No.1300823



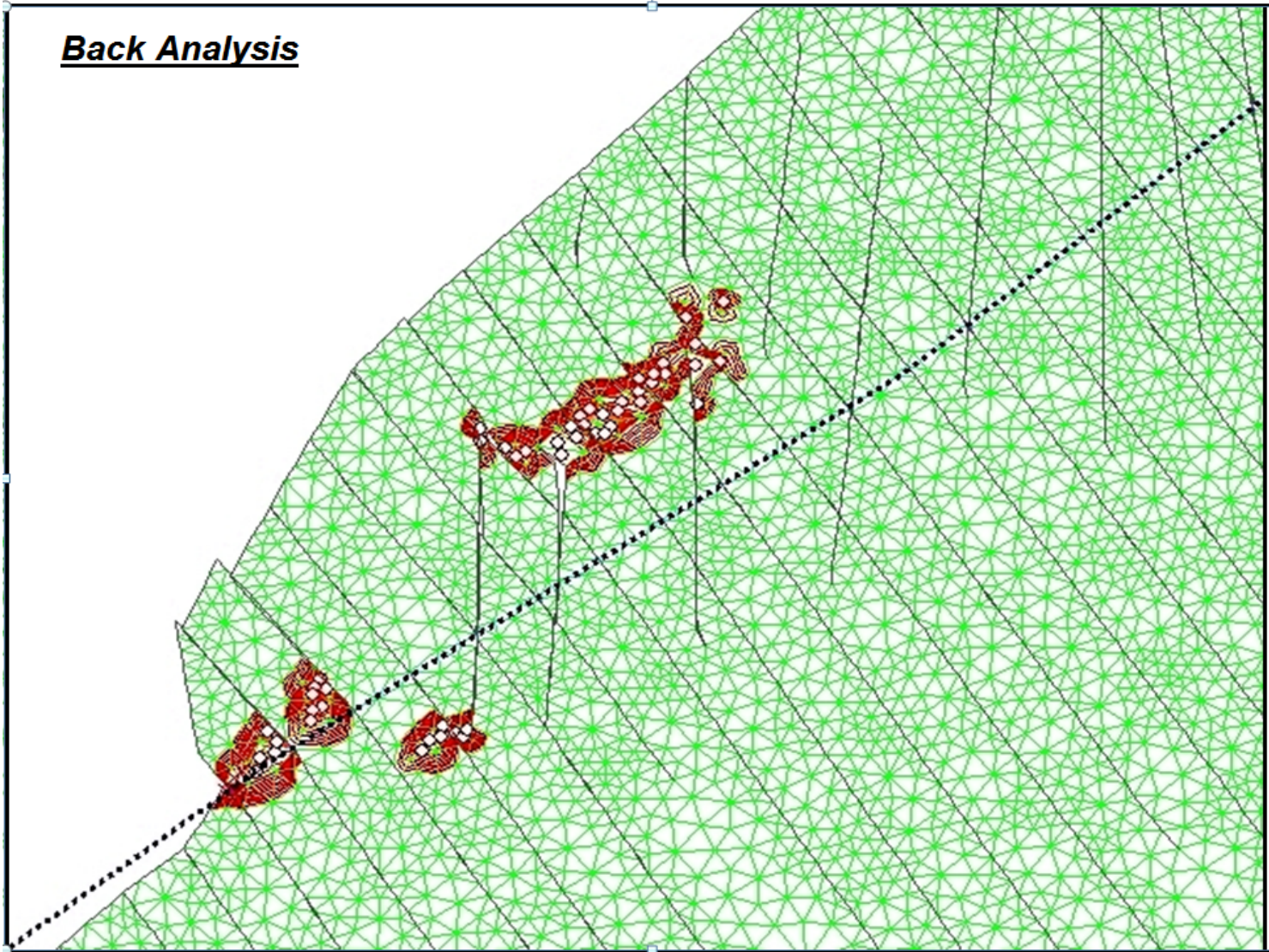
Back Analysis



Tensile Fracturing/Yielded Element Progression to Failure (1 of 4) for Over Steepened Section 6

Figure 27
Project No.1300823

Back Analysis

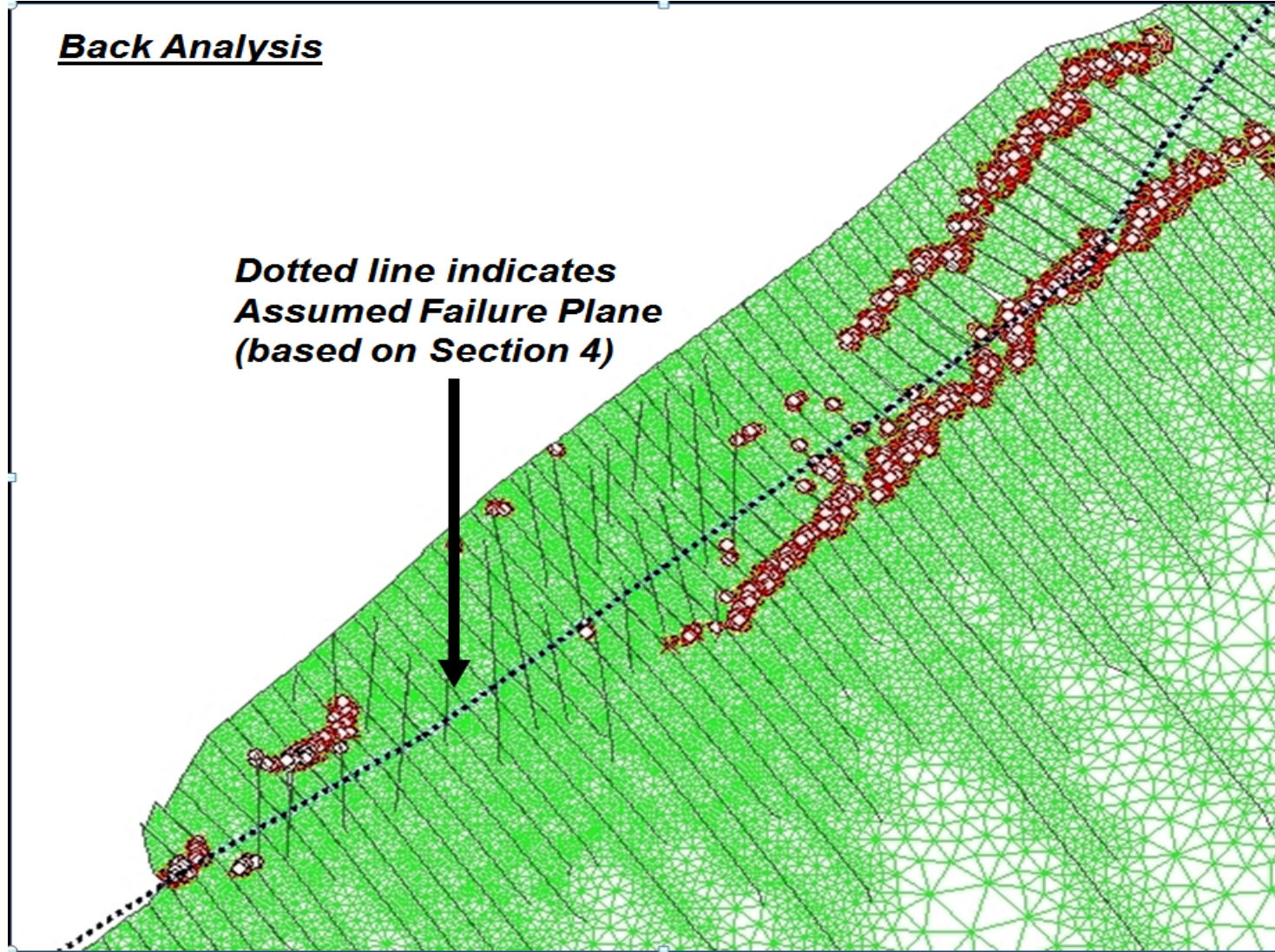


Tensile Fracturing/Yielded Element Progression to Failure (2 of 4) for Over Steepened Section 6

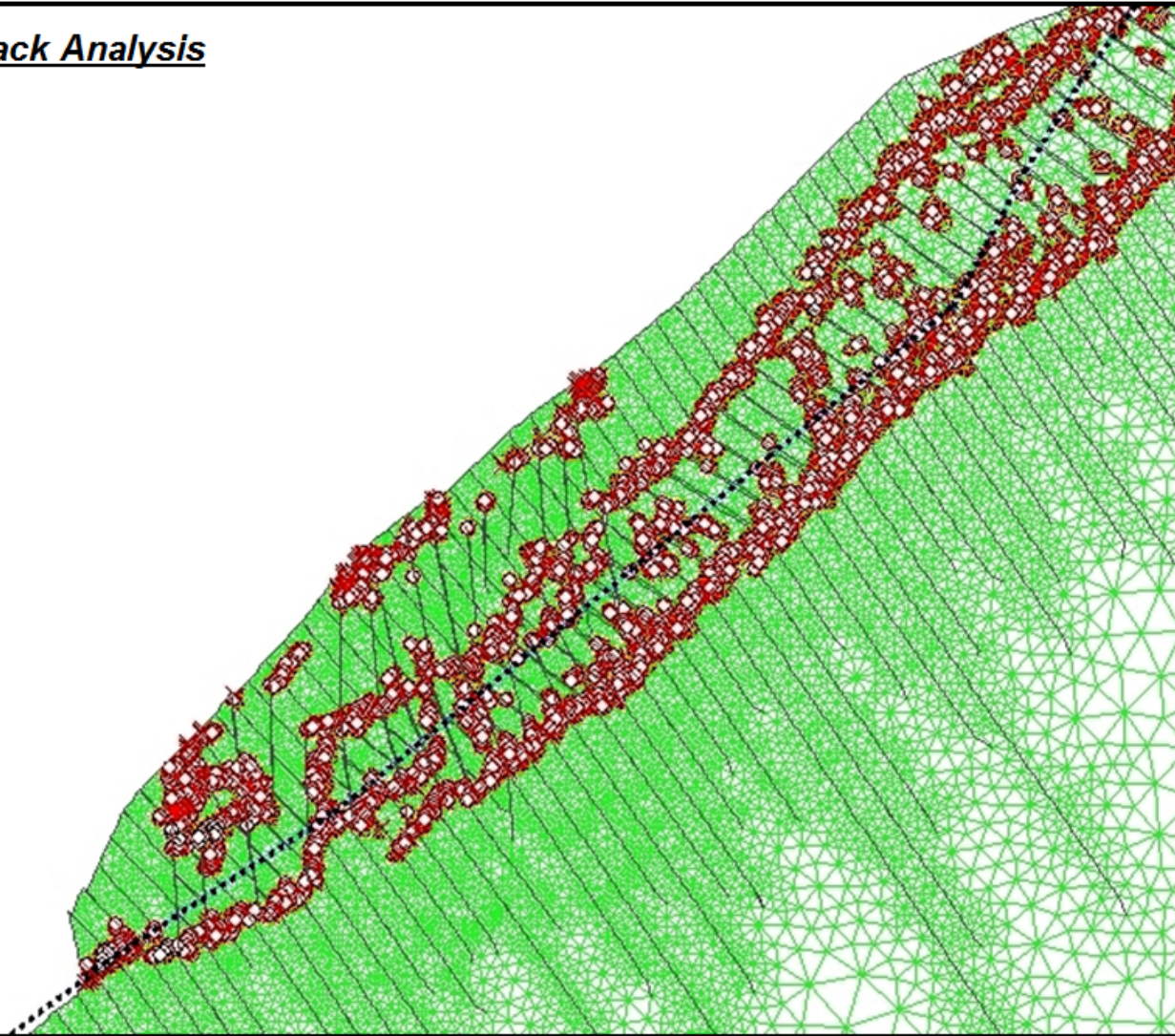
Figure 28
Project No.1300823

Back Analysis

***Dotted line indicates
Assumed Failure Plane
(based on Section 4)***



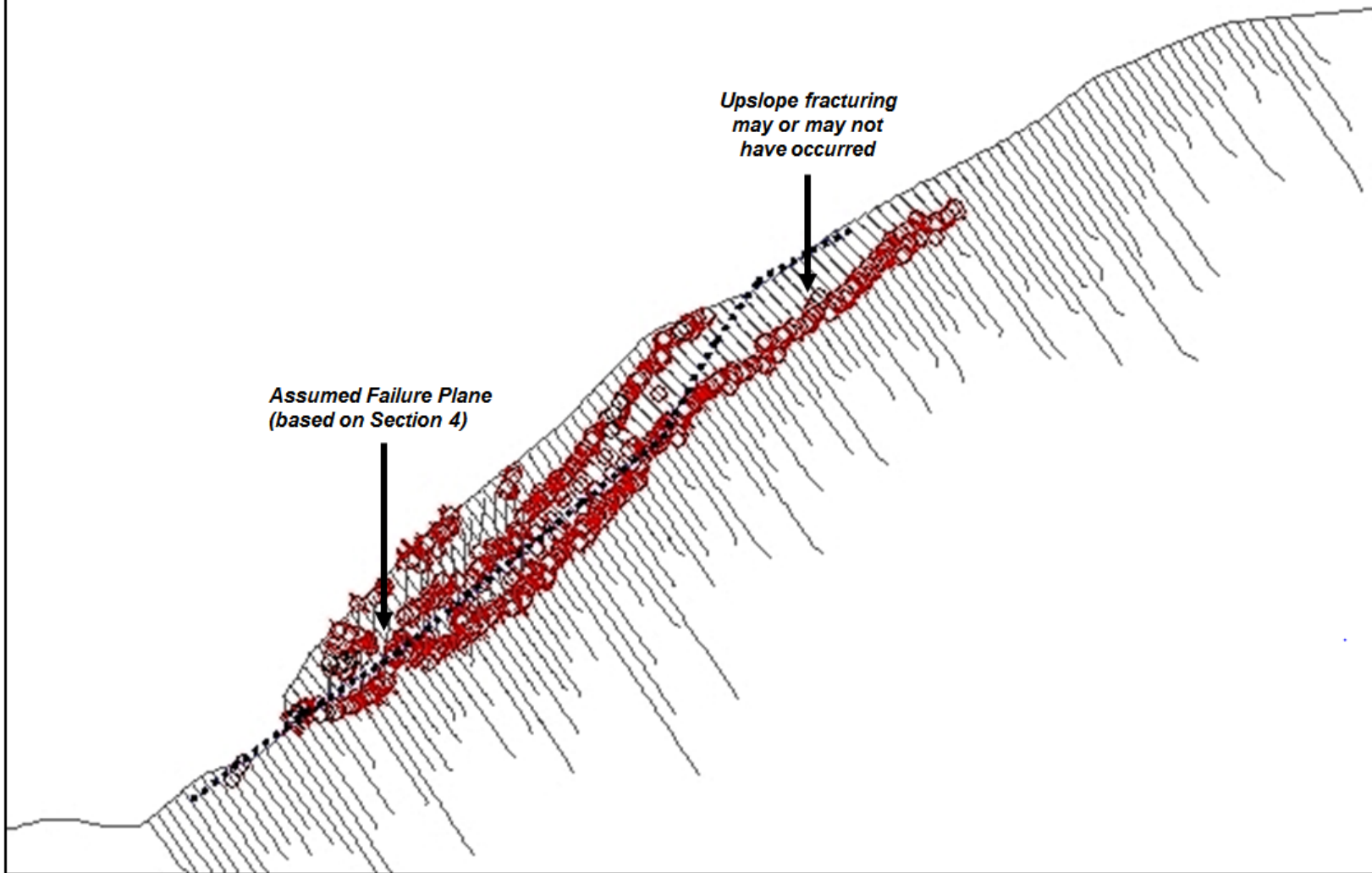
Back Analysis



Tensile Fracturing/Yielded Element Progression to Failure (4 of 4) for Over Steepened Section 6

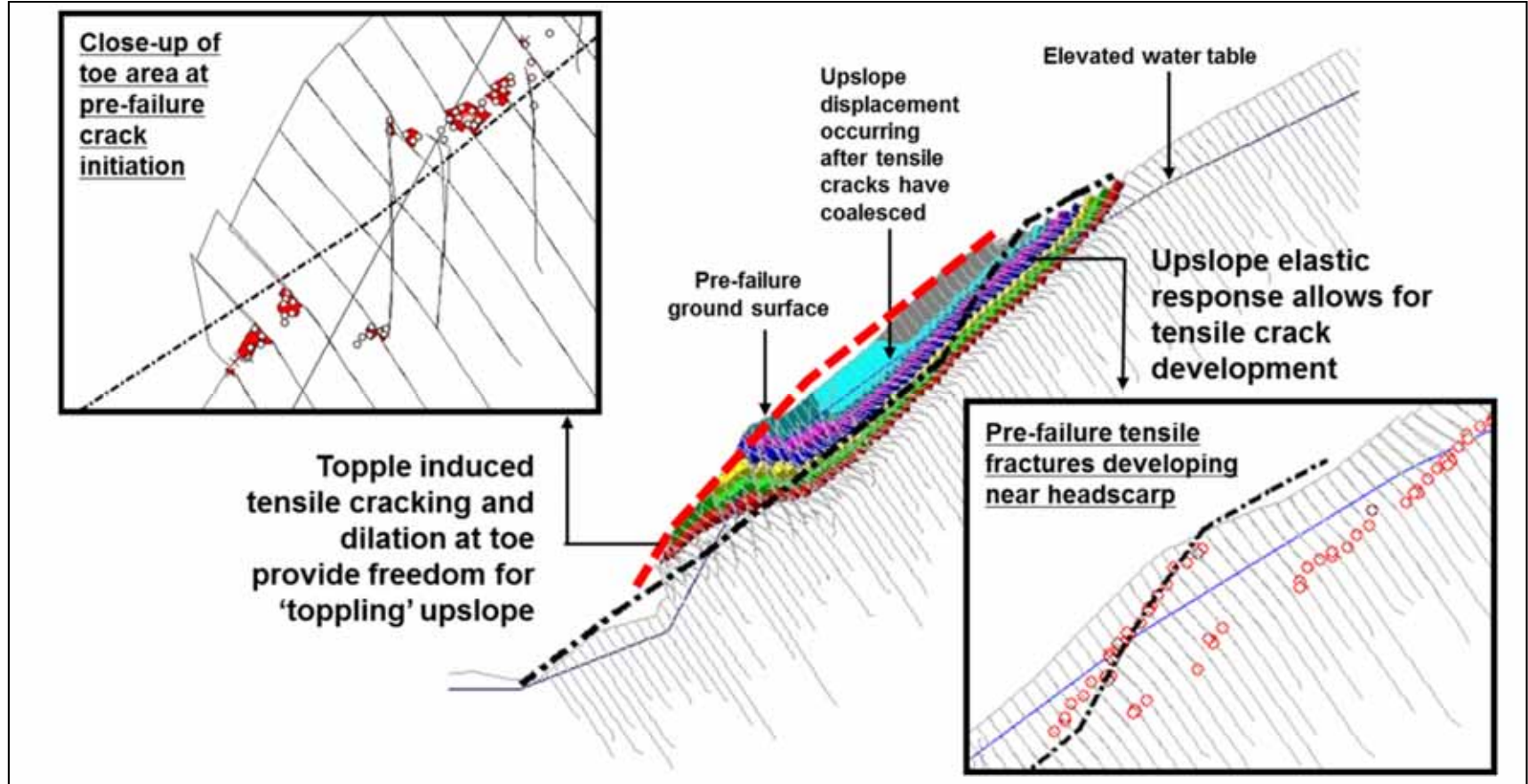
Figure 30
Project No.1300823

Back Analysis

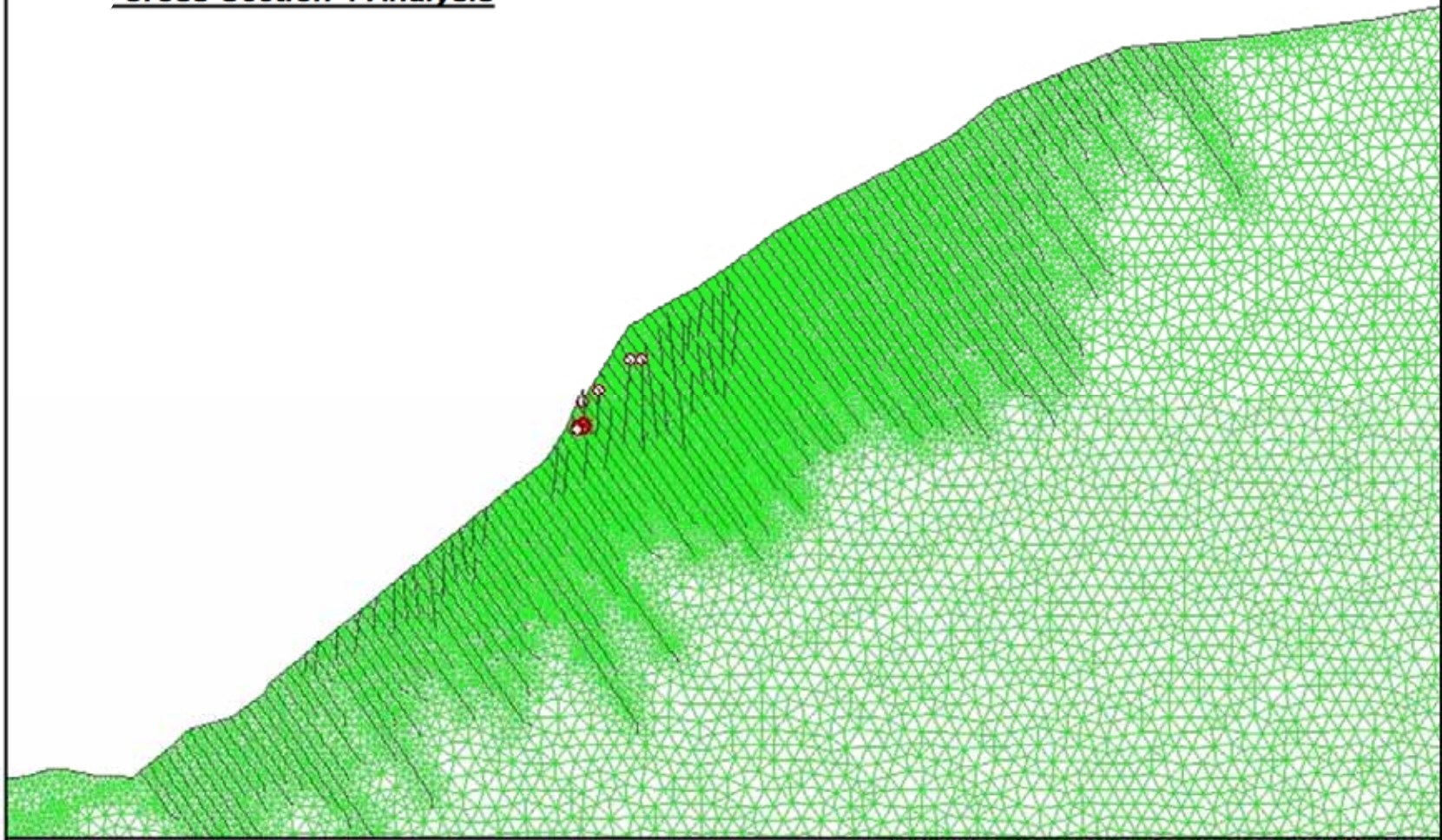


Model Tensile Fracturing and Section 6 on Total Slope Profile

Figure 31
Project No.1300823



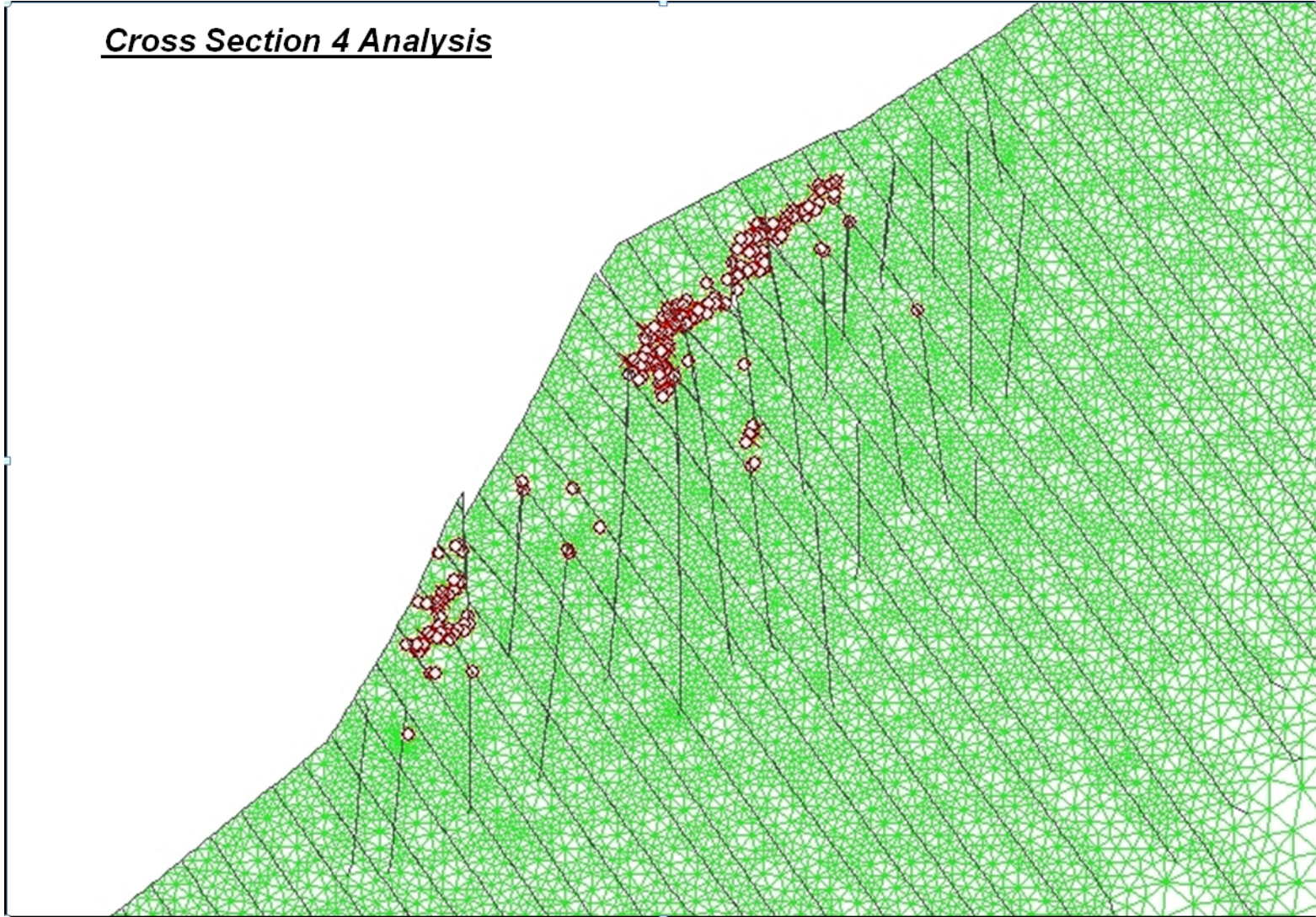
Cross Section 4 Analysis



Tensile Fracturing/Yielded Element Progression to Failure (1 of 5) for Over Steepened Section 4

Figure 33
Project No.1300823

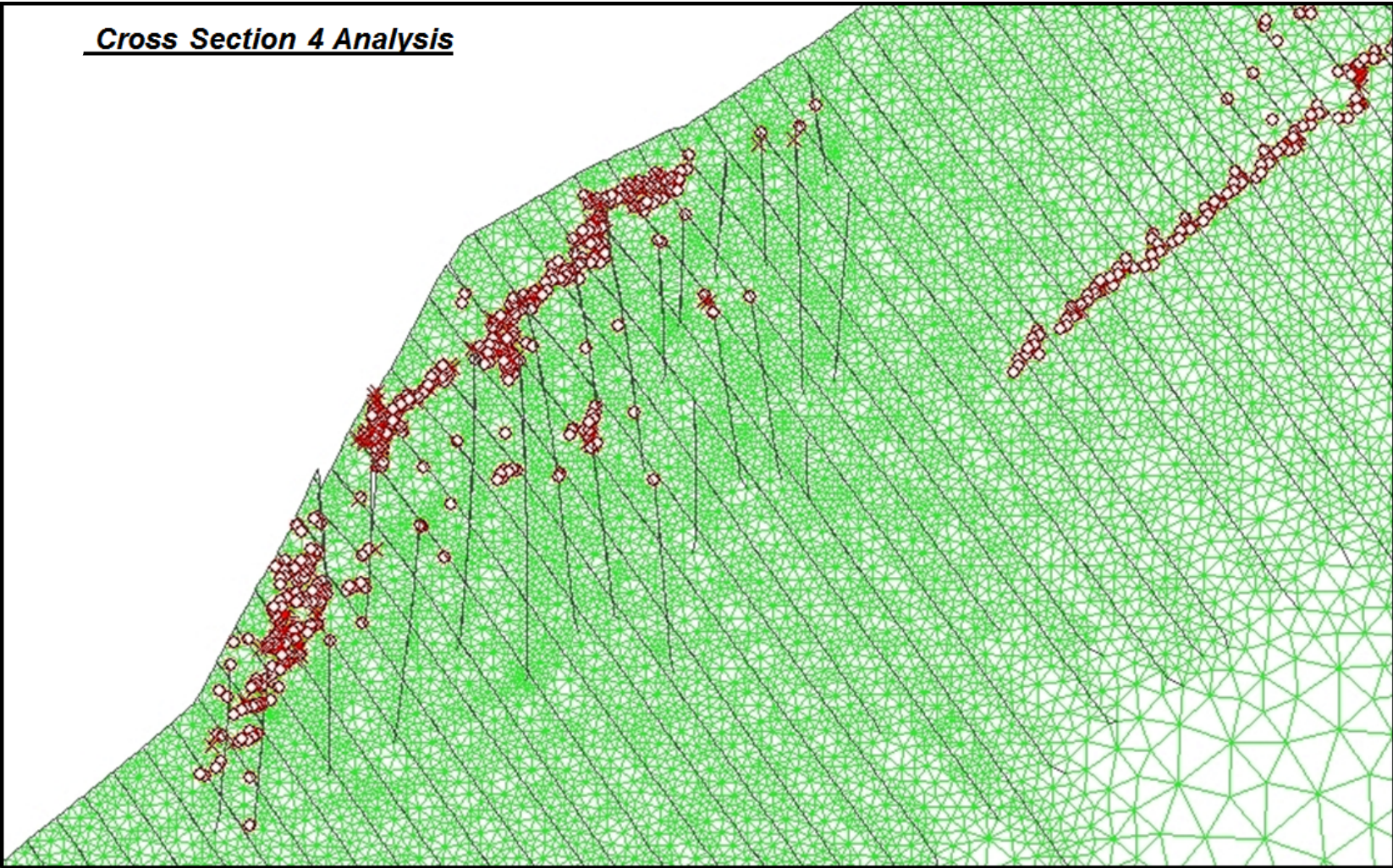
Cross Section 4 Analysis



Tensile Fracturing/Yielded Element Progression to Failure (1 of 5) for Over Steepened Section 4

Figure 34
Project No.1300823

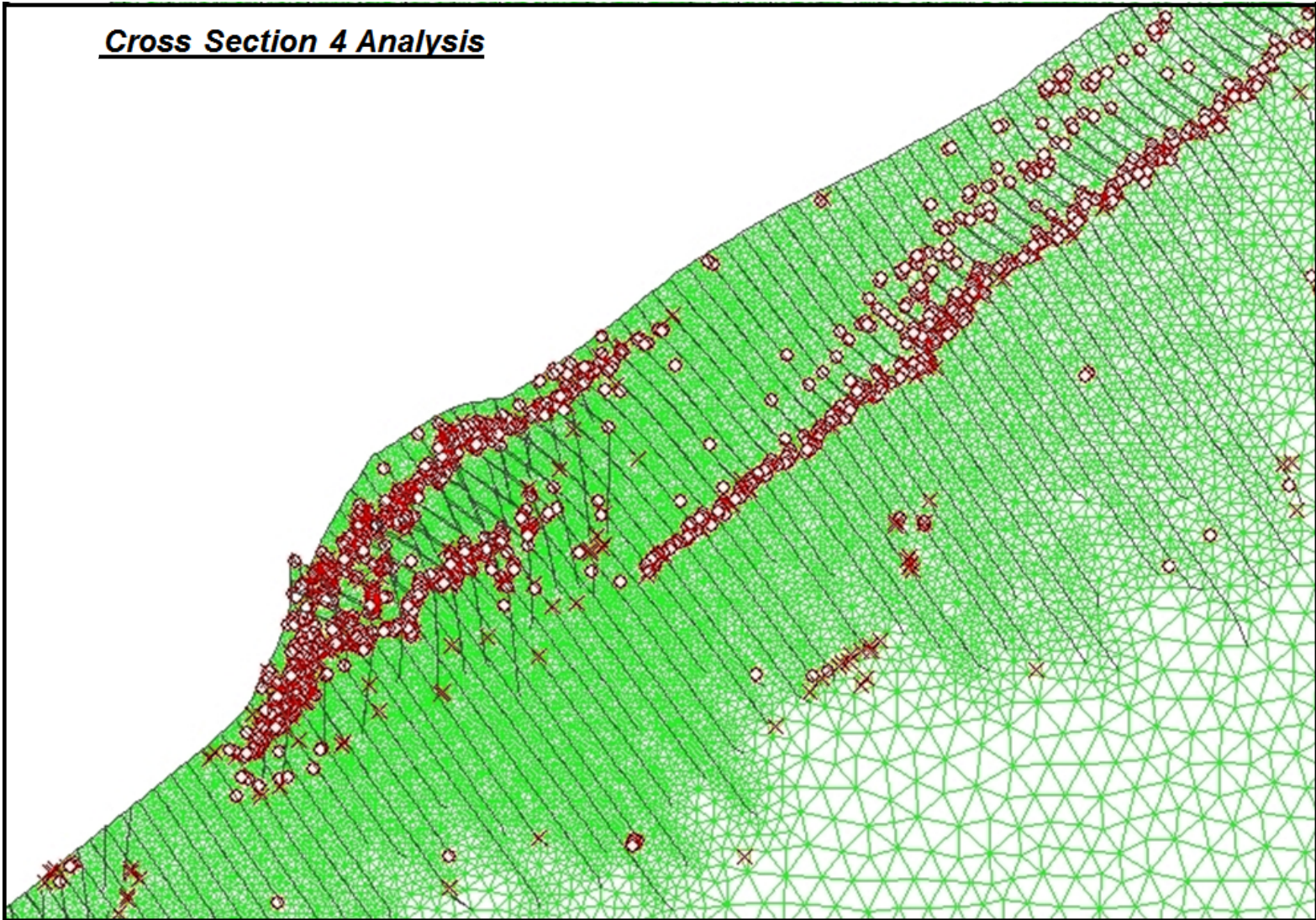
Cross Section 4 Analysis



Tensile Fracturing/Yielded Element Progression to Failure (3 of 5) for Over Steepened Section 4

Figure 35
Project No.1300823

Cross Section 4 Analysis

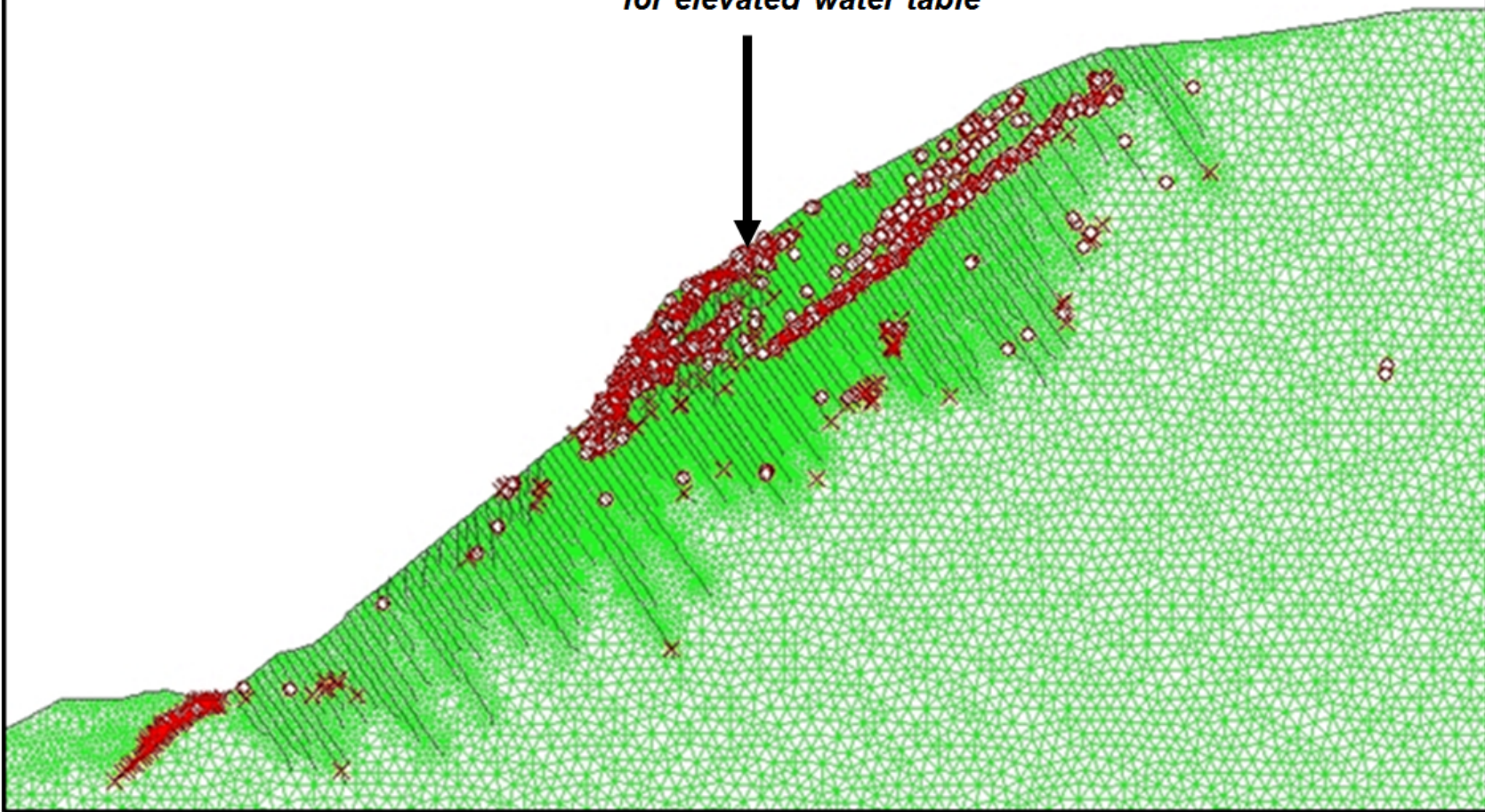


Tensile Fracturing/Yielded Element Progression to Failure (4 of 5) for Over Steepened Section 4

Figure 36
Project No.1300823

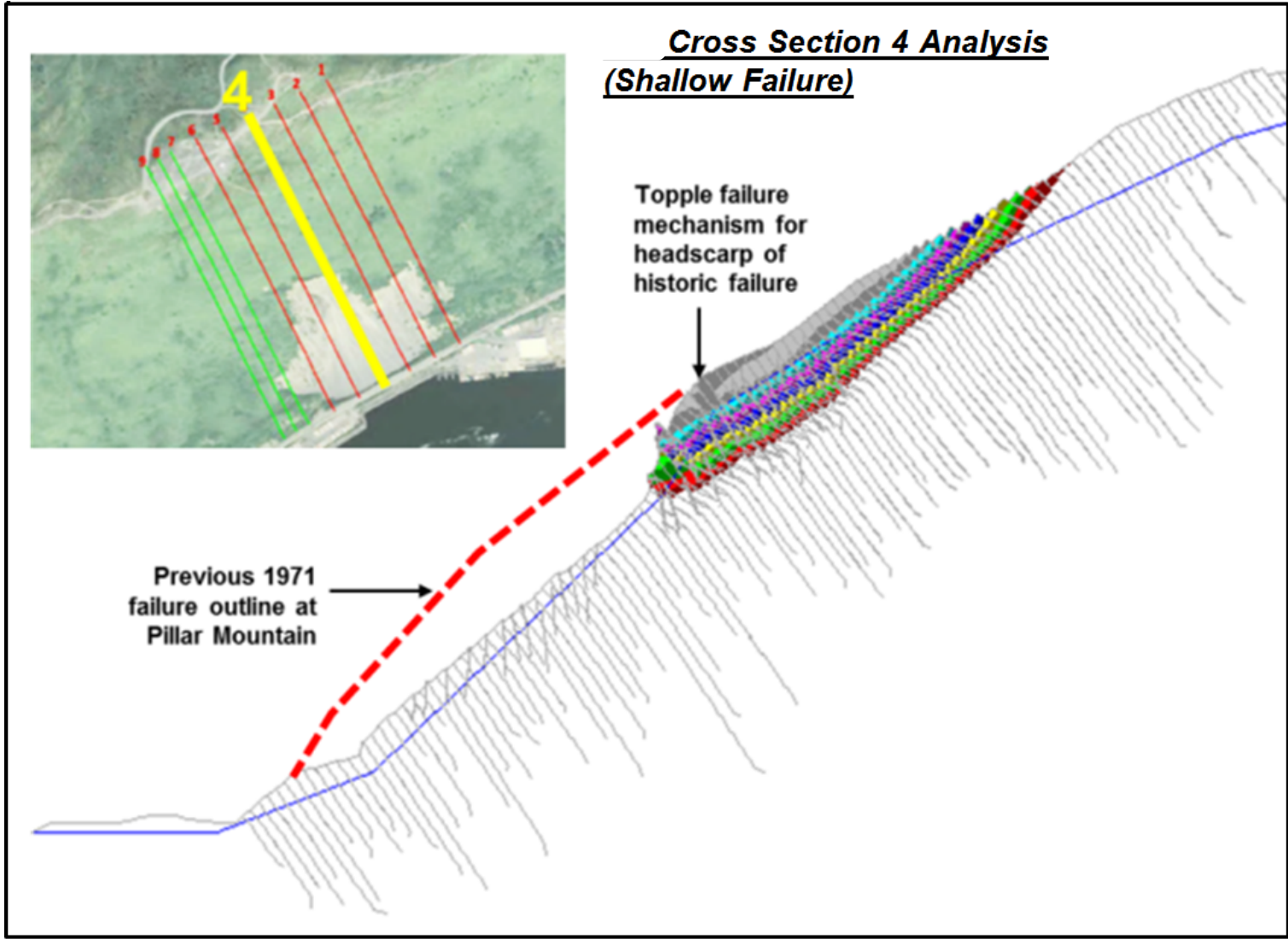
Cross Section 4 Analysis
(Shallow Failure)

*Tensile fractures coalesce at
SSR iteration $1.0 < SSR < 1.3$
for elevated water table*



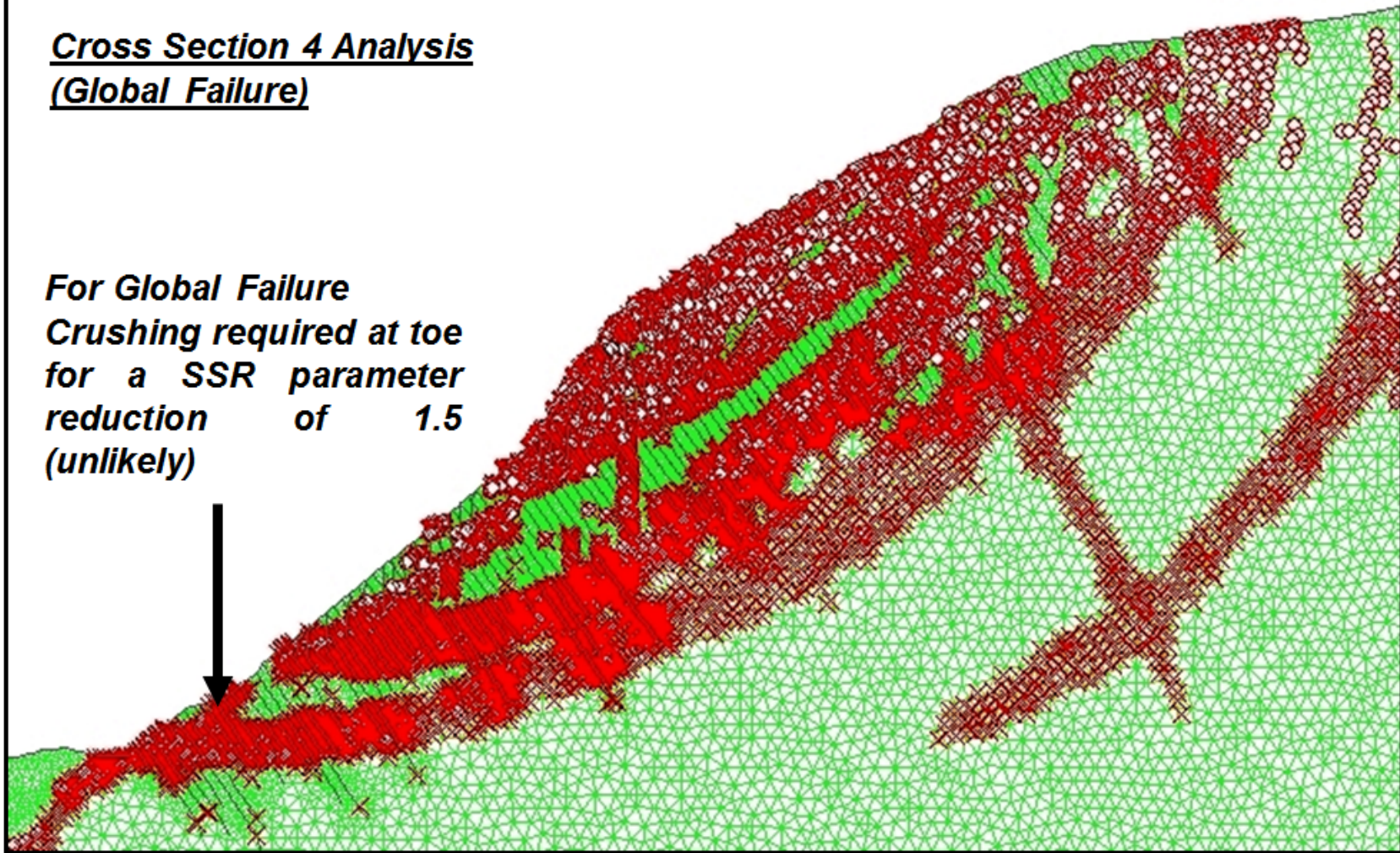
Tensile Fracturing/Yielded Element Progression to Failure (5 of 5) for Over Steepened Section 4

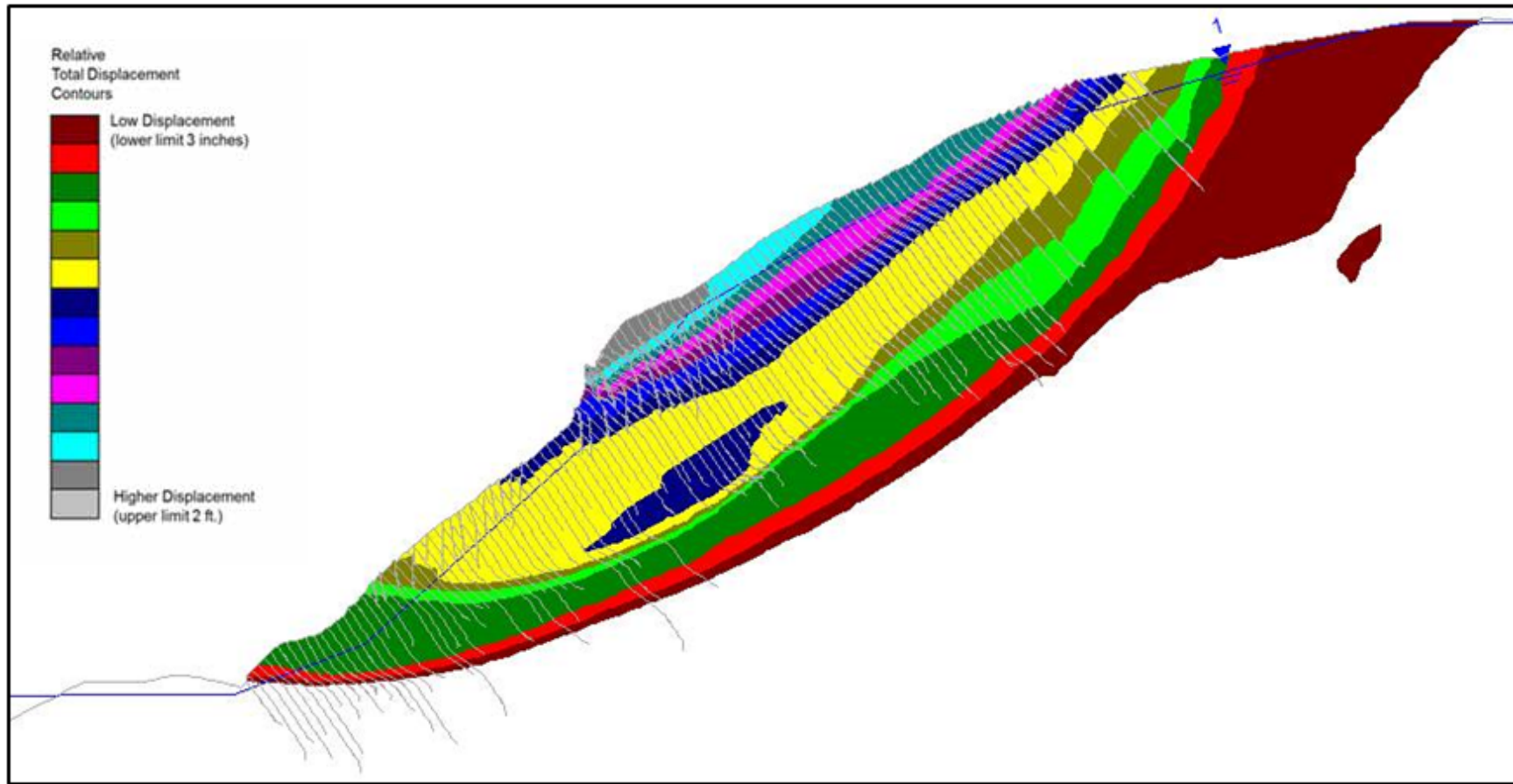
Figure 37
Project No.1300823



Cross Section 4 Analysis
(Global Failure)

For Global Failure
Crushing required at toe
for a SSR parameter
reduction of 1.5
(unlikely)





Calculated Displacement Contours for Cross Section 4
 (color contours shown only to indicate total failure zone)

Figure 40
 Project No.1300823

APPENDIX

Report from Kodiak Mapping Inc

Pillar Mountain Slide Zone

PILLAR MOUNTAIN SLIDE ZONE

KODIAK ALASKA

FINAL LIDAR REPORT

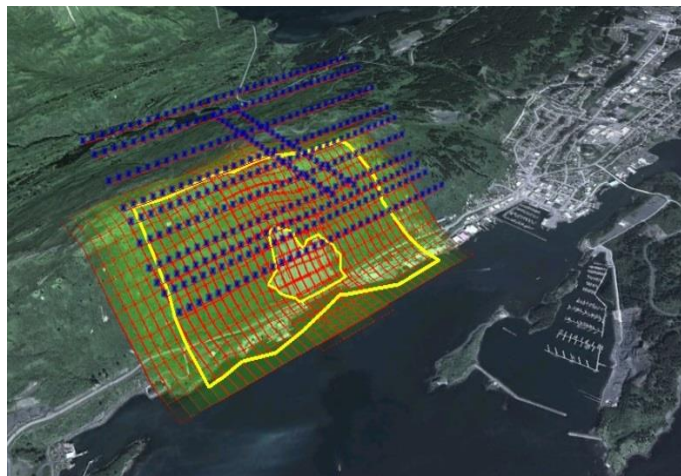
NOVEMBER 5, 2013

PROJECT ABSTRACT



Kodiak Mapping (KMI) was tasked with planning the aerial acquisition of LiDAR and Ortho Photography for the Pillar Mountain slide zone near the City of Kodiak. The area of interest is approximately 2000-ft either side of the landslide scar on the southern face, and extends from the approximate waterline to the summit of the ridge.

LiDAR and Digital Imagery were simultaneously acquired on 18 July 2013 to produce a LiDAR derived Bare Earth Surface in LAS format with approximately 45 – 75 points per meter. Point Density varies throughout the project with more emphasis given to the scar and the steeper faces of the slope. The digital Imagery was utilized to support the generation of a 1.5-inch pixel ortho-photo.



The data acquired is intended to be utilized as a baseline surface for change detection analysis of the Pillar Mountain slide event and its adjacent vicinity. Future datasets can be examined against the baseline model to determine and measure any significant shifts in geological volume or mass feature orientations.

Outlined in this report are the processes and specifications of the baseline surface dataset. Information is provided so that the baseline survey can be replicated in the future for accurate comparison.

LiDAR Collection

LiDAR data with a non-aggregate nominal point density of 25 points per meter was collected on 18 July 2013. Each flight-line was individually terraced up the face of the mountain to account for the dramatic elevation changes in the project area.

The project was flown with flight line side-lap percentages that ranged from 60%- 80% overlap depending on location to increase aggregate point densities in focus areas and to ensure peripheral coverage of near vertical features. The region in the vicinity of the scar exceeds >75-ppm density while areas on the summit of the ridgeline and along the shore have a diminished density of >45-ppm.

Aerial Photography

In addition to the LiDAR data KMI simultaneously collected digital metric quality 4-band imagery. The pixel resolution of the imagery collected during the LiDAR mission is approximately 1.5-inch pixel and was utilized to generate the ortho-photo mosaic.

Project Control

Kodiak Land Surveying was selected as the ground control subcontractor for this project.

A total of 7 ground control Photo ID points were utilized to control the airborne imagery and generate the orthophoto. These same points were utilized as LiDAR QA/QC checkpoints to determine the accuracy and vertical bias of the LiDAR derived surface model.

This ground control can be transferred year to year as the project advances. Additional Ground Control should not be required in later iterations of the change detection project.

KMI utilized the Kodiak CORS to process the airborne vectors for the image triangulation and LiDAR calibration.

Data Processing

Approximately 66 LiDAR production hours were utilized to generate the project deliverables. The majority of production was conducted during the manual edit of the focus areas.

The following automated procedures were performed during the LiDAR edit to help accurately define the Bare Earth surface before manual edit:

Classify Ground:

Max building size: 60 foot

Terrain Angle: 89.00 degrees

Iteration Angle: 18 degrees to plane

Iteration distance: 1.50 to plane

Classify Echo:

Any Intermediate point to Vegetation

Classify Echo:

Any First of Many to Vegetation

Project Deliverables

The following Deliverables were transmitted to Golder and Associates during the course of the project.

- Full frame raw RGB digital images in Tiff format
- Tiled Bare Earth preliminary data in LAS 1.2 format
- Colorized Focus area LiDAR surface in LAS 1.2 format
- Colorized LiDAR tiles merged with focus area dataset: All Points, First return data, and Bare-Earth return in LAS 1.2 format
- Orthophoto Mosaic: Natural Color RGB with a 1.5-inch pixel resolution in Tiff Format.
- Final Project Report

Change Detection

The dataset generated in this iteration of the project will be able to serve as a baseline surface for future iterations of the change detection project.

In future phases of the project a surface generated which replicates similar accuracies can easily be compared to the baseline to detect mass and volume changed throughout the project area. This task can be accomplished with a variety of software packages. KMI would suggest utilizing AutoCAD to import each dataset and compare surface deviations for measurement and analysis.

Project Information

Project Data Acquired: 18 July 2013

Sensor: Riegl VQ-480i

Nominal Flight Altitude: 1000ft AGL

Flight Speed: +/-60kn

Pulse Repetition Rate: 550khz

Nominal Collection Density: 25.6 - 28.1 Points per Meter

Project Average Aggregate: X3

LiDAR vertical Accuracy: 8cm-10cm (Some areas along the sharp vertical inclines resulted in diminished vertical accuracy of 10cm-20cm)

Nominal Vertical Accuracy: Based against the ground survey checkpoints the nominal vertical accuracy of the LiDAR is +/- 0.24-foot

Imagery Sensor: Lieca RCD30 60MP Medium Format Digital Camera System

Raw Imagery Format: RGBN

Processed Imagery Format: RGB

Imagery Resultant Pixel Resolution: 0.12-foot pixel

Project Projection and Datum:

- Horizontal: NAD83, Alaska State Plane Coordinate System, Zone 5
- Vertical: NAVD88, Orthometric Heights based off of Geoid 12A
- Units: Feet

Control Information

CITY OF KODIAK - PILLAR SLIDE PHOTO CONTROL 2013

NOTE: VERTICAL ELEVATION LISTED IS LOCATED AT TOP OF STRUCTURE.

AVG GRND AROUND VAULTS WAS ROUGH AND UNLEVEL.

SEE DESCRIPTIONS FOR ADDITIONAL INFORMATION

GPS static sessions were minimum 1 hr sessions processed through OPUS.

Results = NAD83 (2011)(EPOCH:2010.0000), Alaska State Plain Zone 5 metric

Ortho Heights = NAVD88, GEOID12A metric

Metric - US feet conversion = Blue Marble Geographic Calculator

PointNo.	Northing(Y)	Easting(X)	Elev(Z)	Description
301	1386437.8	1943637.6	1205.2	PHOTO TOP OF VAULT
302	1388199.4	1947473.1	1087.9	PHOTO TOP OF VAULT
303	1386914.3	1945405.1	1193.0	PHOTO TOP OF WOOD PALLET
304	1384486.4	1944257.9	122.2	PHOTO END CORNER WHITE PAINT STRIPE
305	1386274.0	1948506.0	23.6	PHOTO BACK CURB END CORNER PAINT STRIPE
306	1385603.4	1946951.6	19.1	PHOTO END NORTH SIDE YELLOW PAINT STRIPE
307	1386794.1	1944764.1	1236.0	PHOTO TOP OF VAULT

Established in 1960, Golder Associates is a global, employee-owned organization that helps clients find sustainable solutions to the challenges of finite resources, energy and water supply and management, waste management, urbanization, and climate change. We provide a wide range of independent consulting, design, and construction services in our specialist areas of earth, environment, and energy. By building strong relationships and meeting the needs of clients, our people have created one of the most trusted professional services organizations in the world.

Africa	+ 27 11 254 4800
Asia	+ 852 2562 3658
Australasia	+ 61 3 8862 3500
Europe	+ 356 21 42 30 20
North America	+ 1 800 275 3281
South America	+ 56 2 2616 2000

solutions@golder.com
www.golder.com

Golder Associates Inc.
2121 Abbott Road, Suite 100
Anchorage, AK 99507
Tel: (907) 344-6001
Fax: (907) 344-6011



Engineering Earth's Development, Preserving Earth's Integrity

Golder, Golder Associates and the GA globe design are trademarks of Golder Associates Corporation

Established in 1960, Golder Associates is a global, employee-owned organization that helps clients find sustainable solutions to the challenges of finite resources, energy and water supply and management, waste management, urbanization, and climate change. We provide a wide range of independent consulting, design, and construction services in our specialist areas of earth, environment, and energy. By building strong relationships and meeting the needs of clients, our people have created one of the most trusted professional services organizations in the world.

Africa	+ 27 11 254 4800
Asia	+ 852 2562 3658
Australasia	+ 61 3 8862 3500
Europe	+ 356 21 42 30 20
North America	+ 1 800 275 3281
South America	+ 56 2 2616 2000

solutions@golder.com
www.golder.com

Golder Associates Inc.
2121 Abbott Road, Suite 100
Anchorage, AK 99507
Tel: (907) 344-6001
Fax: (907) 344-6011



Engineering Earth's Development, Preserving Earth's Integrity

Golder, Golder Associates and the GA globe design are trademarks of Golder Associates Corporation